nature climate change

LETTERS

https://doi.org/10.1038/s41558-020-0818-9

Check for updates

Fasting season length sets temporal limits for global polar bear persistence

Péter K. Molnár[1,2]✉, Cecilia M. Bitz[3]✉, Marika M. Holland[4], Jennifer E. Kay[5], Stephanie R. Penk[1,2] and Steven C. Amstrup[6,7]

Polar bears (*Ursus maritimus*) require sea ice for capturing seals and are expected to decline range-wide as global warming and sea-ice loss continue[1,2]. Estimating when different subpopulations will likely begin to decline has not been possible to date because data linking ice availability to demographic performance are unavailable for most subpopulations[2] and unobtainable a priori for the projected but yet-to-be-observed low ice extremes[3]. Here, we establish the likely nature, timing and order of future demographic impacts by estimating the threshold numbers of days that polar bears can fast before cub recruitment and/or adult survival are impacted and decline rapidly. Intersecting these fasting impact thresholds with projected numbers of ice-free days, estimated from a large ensemble of an Earth system model[4], reveals when demographic impacts will likely occur in different subpopulations across the Arctic. Our model captures demographic trends observed during 1979–2016, showing that recruitment and survival impact thresholds may already have been exceeded in some subpopulations. It also suggests that, with high greenhouse gas emissions, steeply declining reproduction and survival will jeopardize the persistence of all but a few high-Arctic subpopulations by 2100. Moderate emissions mitigation prolongs persistence but is unlikely to prevent some subpopulation extirpations within this century.

Polar bears occur in 19 subpopulations across four arctic ecoregions[1,2] (Fig. 1). In the southernmost ecoregion (that is, the Seasonal Ice Ecoregion (SIE)), complete sea-ice melt forces bears ashore each summer[1,2], where they rely on body energy reserves for survival and lactation due to the absence of energetically adequate food[5]. Prolonged ice absence from productive continental shelf waters now also forces increasingly long fasts in parts of the other ecoregions (that is, the Divergent Ice Ecoregion (DIE), Convergent Ice Ecoregion (CIE) and Archipelago Ecoregion (AE))[6]—areas where bears historically continued foraging on perennial ice through summer[1]. Although polar bears can fast for months, limits are imposed by the amount of energy bears can store in body reserves before periods of food deprivation[3,5,7]. Lengthening fasts have already lowered body condition, reproduction, survival and abundance in some SIE and DIE subpopulations[8–13], and similar trends are expected throughout the Arctic as ice loss continues[1,2]. However, it remains unclear how long bears can fast before substantial declines in lactation (and therefore cub recruitment) and/or adult survival occur. Information on when such fasting thresholds might be exceeded in different subpopulations, or how rapidly demographic rates would decline following threshold exceedance, is also lacking.

Estimating timelines for the anticipated declines is challenging because data quantifying sea ice–demography relationships are lacking in most subpopulations[2]. Indeed, even in the best-studied subpopulations, abundance projections currently rely on extremely limited data (for example, in the Southern Beaufort Sea, where projections used a threshold of 127 ice-free days to distinguish between good and bad years, based on only 5 years of demographic data[14]). Moreover, today's sea-ice conditions differ substantially from anticipated low ice extremes, thus precluding empirical measurements of how reproduction and survival will change before these changes occur[3]. Previous projections for the future range and abundance of polar bears attempted to overcome such data gaps with expert judgement[1] and/or extrapolations from a few well-studied subpopulations[2], and consequently could only offer limited spatial and temporal forecast resolution with large uncertainties.

Timelines for declining survival and recruitment can be projected, however, even in subpopulations where demographic information is absent, by calculating the energetic needs of fasting polar bears and estimating when longer fasts will preclude meeting those needs[3,15]. Molnár et al. used such energy budget calculations to estimate the likely magnitude of future litter size[15] and adult male survival declines[3] in the Western Hudson Bay subpopulation, but other projections[16,17] incorrectly applied the estimates of Molnár et al., assuming, for example, a universal 180-d persistence threshold, without performing the necessary energy budget calculations, model tests or uncertainty analyses, to justify this choice and/or extrapolations beyond the Western Hudson Bay subpopulation. Here, we describe dynamic energy budget (DEB) estimates of fasting thresholds that limit offspring recruitment and adult survival. We test whether our estimated thresholds capture reported demographic changes in subpopulations where observations are available, project likely timelines for recruitment and survival declines in all SIE, DIE and CIE subpopulations (~80% of Earth's polar bears; Fig. 1) and evaluate the uncertainty surrounding these timelines.

The impacts of fasting on recruitment and survival depend on: the energy reserves of bears at fast initiation; their energy expenditures while fasting; and fast duration. We established baselines for each of these with measurements from bears that were already forced to fast annually for extended periods in the Western Hudson Bay subpopulation (SIE; Fig. 1), and applied sensitivity analyses to these baselines to assess associated uncertainties and

[1]Biological Sciences, University of Toronto Scarborough, Toronto, Ontario, Canada. [2]Ecology and Evolutionary Biology, University of Toronto, Toronto, Ontario, Canada. [3]Atmospheric Sciences MS351640, University of Washington, Seattle, WA, USA. [4]National Center for Atmospheric Research, Boulder, CO, USA. [5]Department of Atmospheric and Oceanic Sciences and Cooperative Institute for Research in Environmental Sciences, University of Colorado Boulder, Boulder, CO, USA. [6]Polar Bears International, Bozeman, MT, USA. [7]Department of Zoology and Physiology, University of Wyoming, Laramie, WY, USA. ✉e-mail: peter.molnar@utoronto.ca; bitz@uw.edu

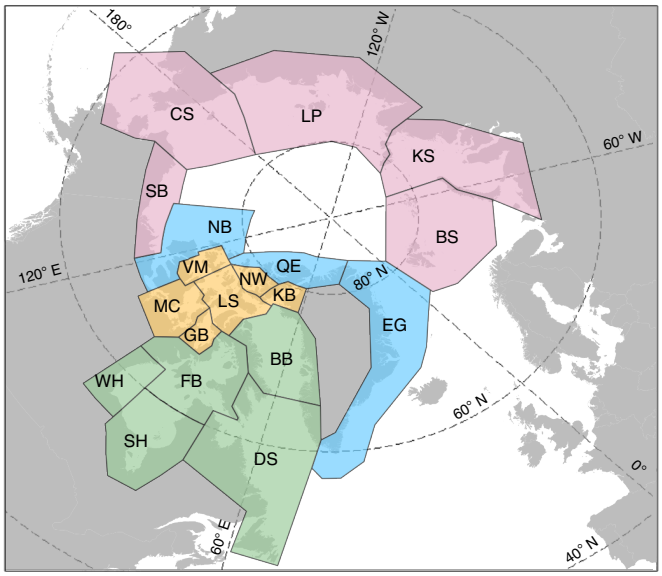

Fig. 1 | Polar bear ecoregions and subpopulations. Ecoregions were defined by temporal and spatial patterns of ice melt, freeze and advection, and by observations of how polar bears respond to those patterns[1]. Subpopulation boundaries follow ref. [1] and include only productive continental shelf waters of the Southern Beaufort Sea to maintain consistency with previous analyses of this subpopulation. Subpopulations in the AE were excluded from our analyses due to inadequate resolution of sea ice in both the PMW and CESM1 (Supplementary Fig. 1). SIE subpopulations (green): BB, Baffin Bay; DS, Davis Strait; FB, Foxe Basin; SH, Southern Hudson Bay; WH, Western Hudson Bay. DIE subpoopulations (red): BS, Barents Sea; CS, Chukchi Sea; KS, Kara Sea; LP, Laptev Sea; SB, Southern Beaufort Sea. CIE subpopulations (blue): EG, East Greenland; NB, Northern Beaufort Sea; QE, Queen Elizabeth Islands. AE (yellow): GB, Gulf of Boothia; KB, Kane Basin; LS, Lancaster Sound; MC, M'Clintock Channel; NW, Norwegian Bay; VM, Viscount Melville Sound.

account for known and potential among-subpopulation differences and within-subpopulation trends. Fast duration was defined as 24 d shorter than the summer period with ice extent below 30% (Extended Data Figs. 1 and 2), with ice extent estimated from passive microwave (PMW) satellite data[18] for the observational period and from large ensemble projections with the Community Earth System Model version 1 (CESM1)[4] for the future (Extended Data Fig. 3). The metabolic requirements of fasting were estimated from mass loss rates observed during the summer on-shore fast in Western Hudson Bay, and a DEB model[3,15] was used to estimate fast duration thresholds beyond which impaired lactation (and hence cub recruitment) and/or adult survival declines are likely (Fig. 2 and Extended Data Fig. 4). Thresholds depend on a subpopulation's distribution of body masses (M_0) and body lengths (L_0) at fast initiation in a given year, $G_{(M_0,L_0)}$(subpop,year), as these variables jointly determine each bear's energy reserves[3]. Data gaps regarding past and present $G_{(M_0,L_0)}$ distributions and the difficulties of reliably anticipating future $G_{(M_0,L_0)}$ (especially for subpopulations not yet experiencing prolonged fasts[3]) were overcome in two steps. First, we established thresholds for the Western Hudson Bay subpopulation during a 1989–1996 reference period ($WH_{89–96}$), using a representative sample of 76 adult males, 41 solitary adult females and 61 (22) females with dependent cubs (yearlings), to estimate $G_{(M_0,L_0)}(WH_{89–96})$ (Fig. 2a–e). Likely thresholds for other time periods and subpopulations were estimated by systematically varying the $G_{(M_0,L_0)}(WH_{89–96})$ baseline (Fig. 2f,g and Table 1) to account for among-subpopulation differences, within-subpopulation trends (Fig. 3) and uncertainties regarding future $G_{(M_0,L_0)}$ distributions (Fig. 4). Model performance was evaluated by intersecting estimated recruitment and survival thresholds with fasting period estimates for 1979–2016 and comparing the resultant demographic impact hindcasts against observations (Fig. 3). Estimates of future demographic impacts were obtained by intersecting projected fasting periods with the full range of biologically feasible impact thresholds, yielding timelines of risk for each subpopulation that account for the uncertainty arising from unknown future $G_{(M_0,L_0)}$ distributions (see below; Fig. 4).

Our DEB model suggests that prolonged fasting impacts cub recruitment first. Survival declines in yearlings, adult males and adult females with offspring follow, while solitary adult females succumb last (Table 1). High rates of recruitment and survival failure following threshold exceedance (Table 1 and Fig. 2) ensure that soon after thresholds are crossed population persistence will be jeopardized. Mother bears cannot fast as long as solitary females due to their reproductive burden; males cannot fast as long as solitary females due to the higher maintenance requirements and lower storage energy of their leaner bodies[3]; and cubs are more vulnerable than yearlings due to their higher reliance on maternal energy reserves[19]. With $G_{(M_0,L_0)}(WH_{89–96})$, for example, impaired cub recruitment is expected when fasts exceed 117 d, followed by declines in yearling recruitment (185 d) and the survival of mother bears (as early as 117 d and no later than 228 d), adult males (200 d) and solitary adult females (255 d) (Table 1, Fig. 2 and Extended Data Fig. 4). These thresholds may vary by months depending on a subpopulation's $G_{(M_0,L_0)}$ (Extended Data Fig. 5), thus also highlighting the inaccuracy of previous projections[16,17] that relied on a universal 180-d threshold.

Model hindcasts capture the timing and nature of observed demographic changes when between-subpopulation differences and within-subpopulation trends in $G_{(M_0,L_0)}$ are accounted for (Fig. 3). For the Western Hudson Bay subpopulation, where lengthening fasts have progressively lowered body conditions[7] and thus impact thresholds (Fig. 3), the DEB model suggests unimpaired recruitment and survival before and during our 1989–1996 reference period but decreased reproductive success since the first crossing of the recruitment impact threshold in the late 1990s (Fig. 3). Hindcasts also suggest stable adult survival during the initial reproductive declines but an increasing likelihood of adult mortalities in recent years: in 2015, the fasting period reached 153 d, approaching the conservatively estimated impact threshold for male survival (now ≤171 d; Fig. 3), and possibly also for the survival of females with offspring (between 98 and 192 d in 2007; now possibly lower; Fig. 3). Rates and timelines of actual and modelled declines mirrored one another, with the Western Hudson Bay subpopulation transitioning from high recruitment during the 1980s to declines in juvenile, subadult and senescent adult survival in the late 1990s/early 2000s, while prime-age adult survival remained unaffected[8] (Fig. 3). It remains unclear whether the resulting ~22% abundance decline[8] has continued in recent years or whether the population may have temporarily stabilized at a lower abundance[12,20], but recruitment remains low[20] and female survival appears to have decreased in recent low-ice years[12,20], as hindcasted (Fig. 3). Male survival also may have declined, but limitations of the most recent census prevented disentangling fasting-related and other mortalities[12].

Elsewhere in the SIE, bears are of similar length[21,22] but greater mass[23] than in the Western Hudson Bay subpopulation, possibly because of shorter ice-free periods (Foxe Basin and Baffin Bay; Fig. 3), comparatively later ice break-ups that allow for additional pre-fast foraging opportunities (Southern Hudson Bay and Foxe Basin)[24] and/or an increasing availability of harp seals (*Pagophilus groenlandicus*) (Davis Strait and Baffin Bay)[25,26]. Nonetheless, body mass declines similar to those in the Western Hudson Bay subpopulation have occurred throughout the SIE[10,13,27], except possibly

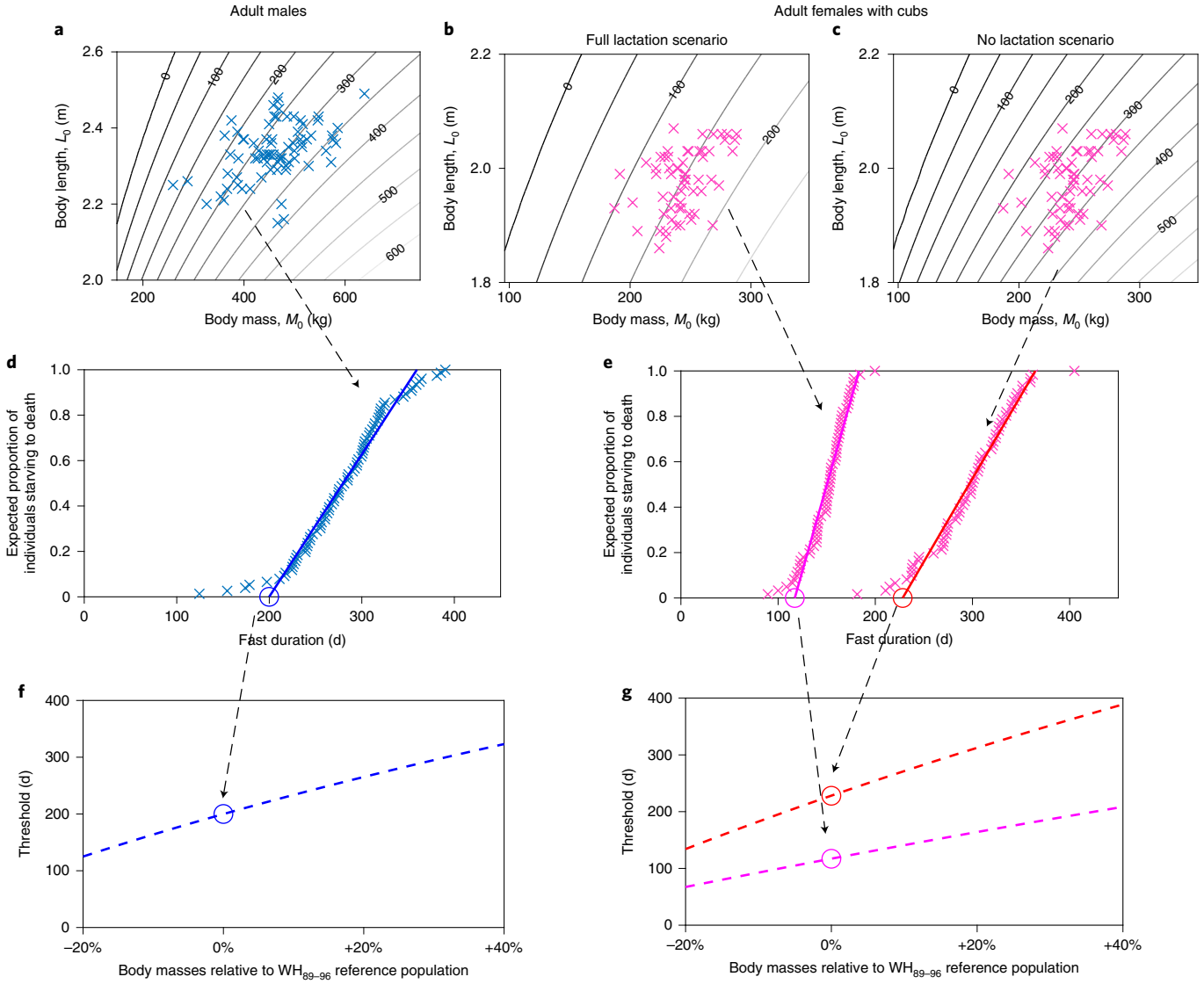

Fig. 2 | Method for estimating fasting impact thresholds beyond which cub recruitment and adult survival begin to decline rapidly. Thresholds were estimated by calculating the maximum number of fasting days that polar bears can survive, given their metabolic requirements and fast-initiating energy reserves. Arrows illustrate the logical flow of our analyses, progressing from individual samples to population-level threshold estimates. Threshold calculations are shown for adult males and adult females with cubs. Calculations for solitary adult females and females with dependent yearlings were performed the same way (Extended Data Fig. 4). **a**–**c**, Fast-initiating masses and lengths of adult males (**a**; blue crosses) and adult females with cubs (**b** and **c**; magenta crosses) in $WH_{89–96}$, relative to DEB estimates of the number of days to death by starvation (contour lines). Due to lacking data on how starvation impacts lactation, we estimated starvation times for females with cubs for two extreme strategies of reproductive investment that bracket the true time to female death: full lactation until death (**b**) and no lactation when fasting (**c**). **d**,**e**, Cumulative distributions of the estimated starvation times shown in **a**–**c**. *X*-intercepts (circles) of linear fits to the 5th to 95th percentiles of these distributions (solid lines) indicate: (**d**) a survival impact threshold for adult males (200 d) beyond which mortality increases by ~0.6% for each additional fasting day (regression slope); and (**e**) lower (magenta) and upper (red) estimates for the survival impact thresholds of females with cubs (117–228 d). In **e**, the lower estimate doubles as a recruitment impact threshold as longer fasts are only possible with reduced lactation, and thus compromised cub condition, growth and survival. **f**,**g**, Sensitivity analyses corresponding to **d** and **e**, respectively, illustrating the dependence of impact thresholds on the fast-initiating masses of bears, obtained by adjusting all $WH_{89–96}$ masses upwards or downwards by a specified percentage within biologically reasonable bounds.

in Foxe Basin where stability is assumed[28]. After adjusting impact thresholds accordingly, our model hindcasts suggest modest but persistent reproductive impacts in Southern Hudson Bay since the late 1990s, larger reproductive impacts in Davis Strait, potential reproductive impacts in Baffin Bay, no reproductive impacts in Foxe Basin and no impacts on adult survival anywhere (Fig. 3). In agreement with simulations, females in Southern Hudson Bay appear to be sacrificing their body condition to maintain lactation[13], and cub survival also has declined in recent years[24]; in Davis Strait, cub recruitment is among the lowest of all SIE subpopulations while adult survival nevertheless remains high[25]; in Baffin Bay, offspring recruitment has decreased since the mid-1990s while adult survival has remained stable[27]; and in Foxe Basin, no demographic impacts are apparent[28].

Model hindcasts are more difficult to evaluate for the DIE and CIE, where a lack of sampling (Kara Sea, Laptev Sea, East

Table 1 | Fasting impact thresholds for polar bear recruitment and survival

Bear class	Recruitment impact threshold (number of fasting days)				Survival impact threshold (number of fasting days)				Estimated decrease in survival for each additional fasting day beyond the survival impact threshold
	−20%	0%	+20%	+40%	−20%	0%	+20%	+40%	
Adult males	NA	NA	NA	NA	125	200	265	323	−0.6% per day
Solitary adult females	NA	NA	NA	NA	158	255	342	420	−0.4% per day
Adult females with cubs	67	117	164	208	LB: 67	LB: 117	LB: 164	LB: 208	
					UB: 134	UB: 228	UB: 313	UB: 389	−0.7% per day
Adult females with yearlings	108	185	255	320	LB: 108	LB: 185	LB: 255	LB: 320	
					UB: 138	UB: 232	UB: 317	UB: 394	−0.8% per day

Four estimates are shown for each bear class and threshold, corresponding to scenarios where bears begin fasting 20% lighter (−20% threshold), the same (0% threshold), 20% heavier (+20% threshold) or 40% heavier (+40% threshold) than $WH_{89–96}$ bears. Body conditions at the +40% limit are considered unrealistically high, but were included as a maximum conceivable upper bound under perfect conditions (see Extended Data Fig. 7). Due to uncertain energetic investment into lactation, the true survival impact threshold could only be bounded for females with dependent offspring (see Fig. 2e,g). LB, lower bound; UB, upper bound.

Greenland and Queen Elizabeth Islands) or predominantly spring sampling (Southern Beaufort Sea, Chukchi Sea, Barents Sea and Northern Beaufort Sea)[11,29,30] prevented reliable estimation of fast-initiating (late-summer) $G_{(M_0,L_0)}$ distributions[3,15] and, thus, of subpopulation-specific impact thresholds. Nonetheless, DEB hindcasts suggest possible declines in recruitment and, perhaps, adult survival for the Southern Beaufort Sea, Chukchi Sea, Kara Sea and Barents Sea from as early as the 1990s—if bears in these subpopulations are more reliant on a stable ice cover for hunting (Extended Data Fig. 6a), move more during fasting, and/or are lighter (lower energy reserves), longer (higher metabolic requirements), or both, than $WH_{89–96}$ bears (Fig. 3). Correspondingly, in the Southern Beaufort Sea subpopulation (characterized by declining body conditions[9], possibly greater skeletal sizes[21], additional movement costs imposed by ice fragmentation and drift during on-ice fasting[31]), both recruitment and survival (both sexes and all age classes) decreased with recent low ice, causing a 25–50% abundance drop[11]. In contrast, in the neighbouring Chukchi Sea subpopulation, demographic declines have not yet occurred[29], consistent with model outcomes for the reported good body conditions that are maintained by extraordinary marine productivity[29]. The Barents Sea subpopulation currently seems stable but with low recruitment[32], consistent with the energetic requirements of bears that are shorter but also lighter than $WH_{89–96}$ bears[23] (Fig. 3 and Extended Data Fig. 5), and no impacts have been observed in the Northern Beaufort Sea[30], as simulated (Fig. 3).

For estimates of future demographic impacts, we acknowledge but do not resolve uncertainties[3,15] regarding future subpopulation-specific $G_{(M_0,L_0)}$ distributions. Instead, we estimated fasting impact thresholds for the full range of biologically feasible $G_{(M_0,L_0)}$ (Extended Data Fig. 7), assuming that bears may begin fasting 20% lighter, the same, 20% heavier, or 40% heavier than $WH_{89–96}$ bears (henceforth, the −20%, 0%, +20% and +40% thresholds; Table 1). Intersecting these thresholds with projected annual fasting periods under business-as-usual (Representative Concentration Pathway to 8.5 Wm^{-2} (RCP8.5)) or mitigated (RCP4.5) scenarios[33] yields timelines of risk for when recruitment and survival will likely begin declining (Fig. 4 and Extended Data Fig. 8): when fast duration remains below the −20% threshold in a subpopulation, we consider demographic impacts unlikely because short fasts are typically associated with good body conditions[7,9,13]; based on the observed impacts in the SIE and DIE (Fig. 3), we suggest that demographic impacts are likely to appear between exceedance of our −20% and +20% thresholds; and because high body conditions cannot be maintained with long fasts, effects become inevitable by the time the +40% threshold is crossed (Extended Data Fig. 8). Timeline uncertainties, arising from uncertainty in DEB parameters and uncertain ice availability–fasting relationships, were dealt with by evaluating how the timelines of risk would shift if our baseline assumptions were violated (Extended Data Figs. 6 and 9).

Estimated timelines of risk are shown in Fig. 4, illustrating how the physiological limits of fasting determine the polar bear's fate with unmitigated greenhouse gas emissions. Unlike previous projections that suggest ultimate large-scale declines but do not provide explicit timelines[1,2], our DEB approach provides previously unavailable mechanistic underpinnings that capture past demographic changes and quantify the timing, nature, order, and uncertainty surrounding future changes—even for data-scarce subpopulations. Despite timeline uncertainties, it is evident that demographic impacts will worsen in already affected subpopulations, and that similar impacts will occur over most of the species' range (Fig. 4). By 2100, following the RCP8.5 scenario, recruitment will be severely compromised or impossible everywhere except perhaps in the Queen Elizabeth Islands subpopulation. Most subpopulations will also experience dramatically increased adult mortality, making persistence unlikely throughout most of the polar bear range (Fig. 4). Ultimately, aggressive greenhouse gas emissions mitigation will be required to save polar bears from extinction, but moderating emissions to RCP4.5 would slow progressive extirpation, probably allowing some subpopulations to persist through this century—albeit with reduced recruitment (Fig. 4).

Potential errors and uncertainties remain with respect to the exact onset of demographic declines, both because of our reliance on a single Earth system model and because of uncertainties and variations in bear behaviour and energy usage among subpopulations. If many Earth system models were employed rather than just one, we would expect an increase in accuracy, but also an increase in uncertainty from accounting for structural uncertainty in Earth system model parameters and physics that we currently neglect. However, in the work presented here, the uncertainty in the onset of demographic declines is dominated by biological uncertainties, which is why we accept the underestimated uncertainty of fast durations that stems from using only one Earth system model at this time. More field data on polar bear characteristics could allow us to better constrain DEB model parameters, thereby increasing accuracy and reducing uncertainty in the demographic estimates, but filling these data gaps will probably not lead to more optimistic conclusions. Impacts could potentially occur decades sooner

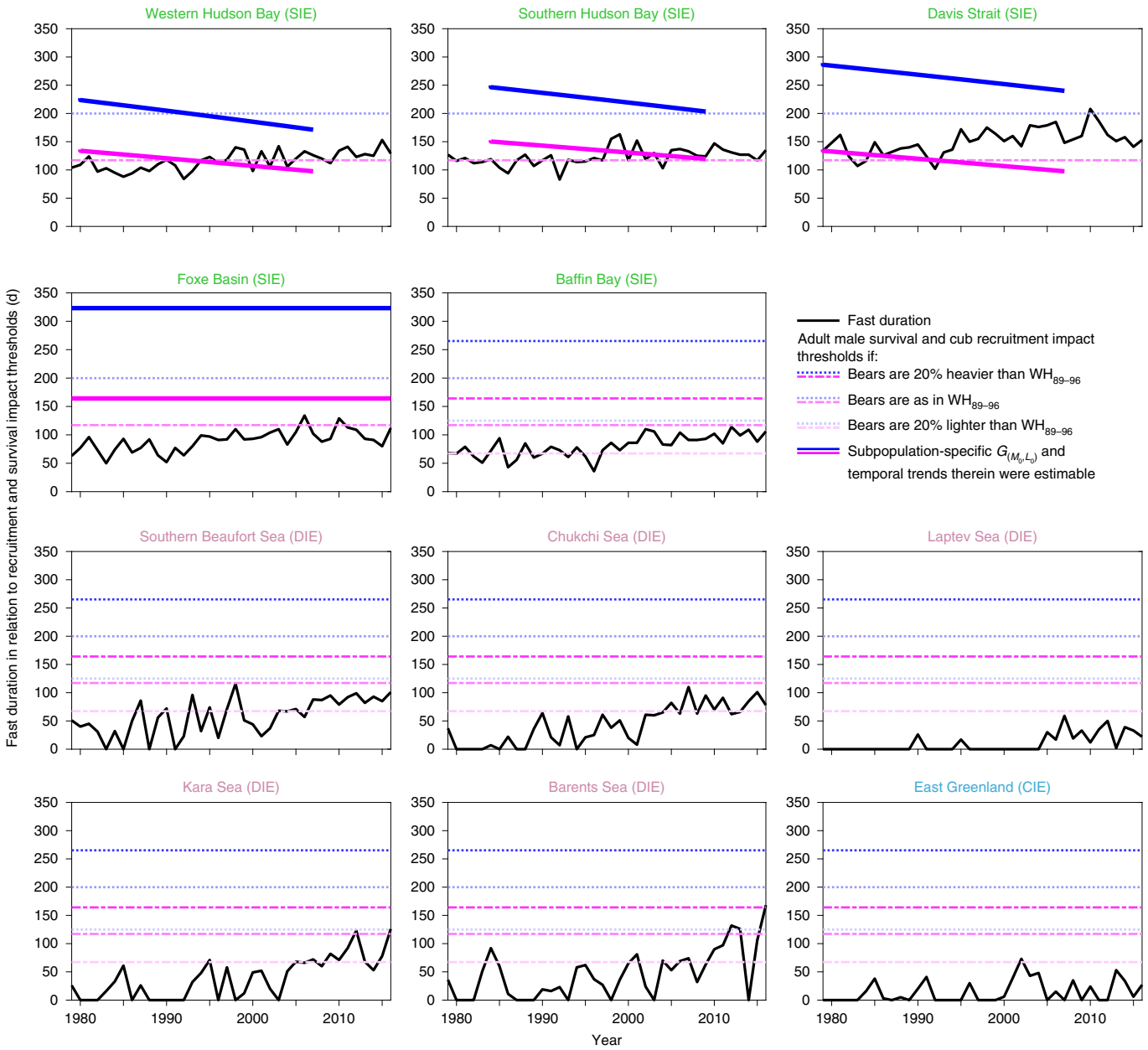

Fig. 3 | Estimated annual fasting period lengths of polar bears in the SIE, DIE and CIE from 1979–2016, in relation to estimated cub recruitment and adult male survival impact thresholds. For subpopulations where body lengths and fast-initiating body masses were estimable (Western Hudson Bay, Southern Hudson Bay, Davis Strait and Foxe Basin), we calculated subpopulation-specific impact thresholds by adjusting the $G_{(M_0,L_0)}$($WH_{89\text{-}96}$) baseline (dot-dashed magenta line for recruitment; dotted blue line for adult male survival) for among-subpopulation differences and within-subpopulation trends in body mass[7,10,13,28] (thick solid magenta and blue lines). In the Western Hudson Bay subpopulation, for example, body masses declined by ~5.7% per decade during 1980–2007 (ref. [7]), leading to corresponding declines in the adult male survival (227 d in 1980; 171 d in 2007) and recruitment impact thresholds (136 d in 1980; 98 d in 2007). For subpopulations where fast-initiating masses and lengths were inestimable, we show a series of impact thresholds for cub recruitment (dot-dashed magenta) and adult male survival (dotted blue) for reference, assuming body masses that are 20% lower (light shade), the same (medium shade) or 20% higher (dark shade) than in $WH_{89\text{-}96}$. Fasting period lengths (solid black lines) were estimated as 24-d shorter than the summer period with ice extent <30%, and bears were assumed to be conserving energy while fasting, as observed in Western Hudson Bay. Recruitment and adult male survival declines are expected when the fasting period length exceeds the corresponding impact threshold. Impact thresholds for yearling recruitment and the survival of mother bears are not shown, but are similar to those for adult male survival (Table 1), and may thus also have been crossed occasionally in some SIE and DIE subpopulations in recent years. Only East Greenland is shown for the CIE, as the Northern Beaufort Sea and Queen Elizabeth Islands subpopulation regions have retained a perennial ice cover to date. Font colours of subpopulation names correspond to their ecoregion designation: green, SIE; red, DIE; blue, CIE.

than projected in Fig. 4 (Extended Data Figs. 6c and 9c), because all DEB model parameters and assumptions were chosen to yield optimistic threshold estimates in cases where data scarcity necessitated a choice. For example, we assumed that all bears follow an energy-conserving strategy of limited movement during fasting, as is observed in Western Hudson Bay, but higher movement costs combined with low hunting success may in some subpopulations drive bears into energy deficits well before they are forced to

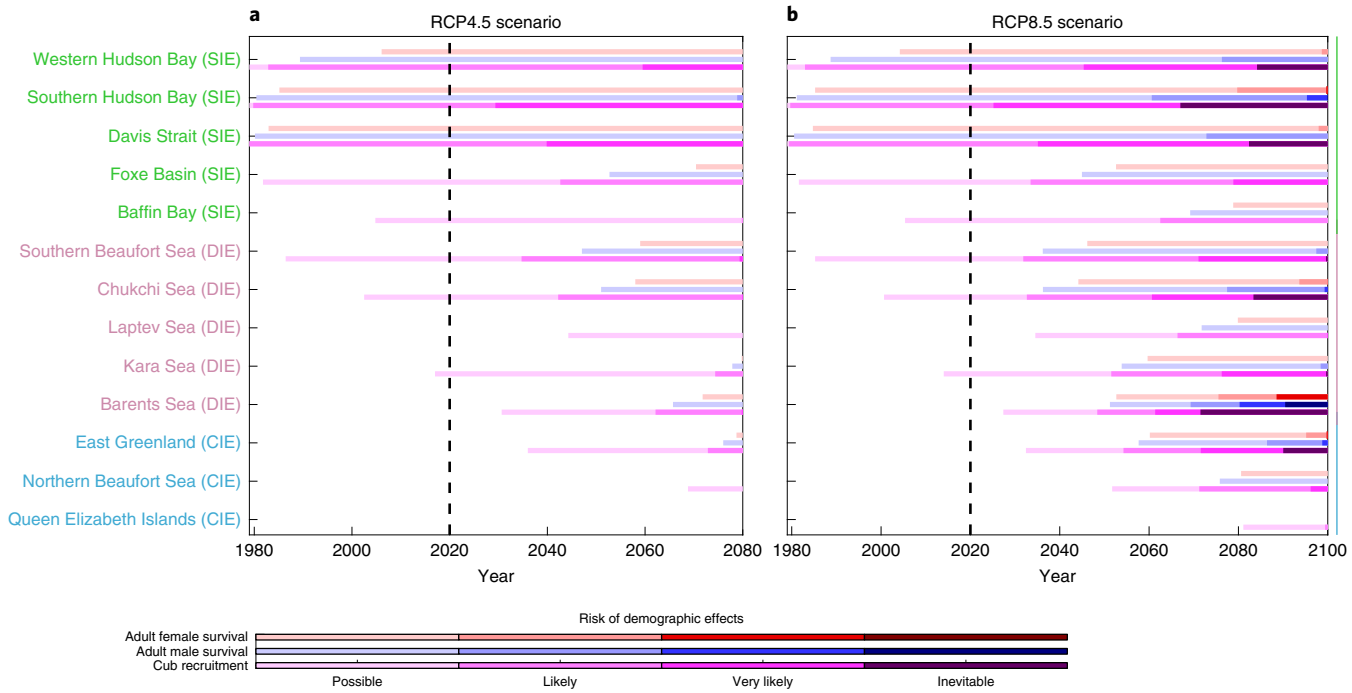

Fig. 4 | Modelled timelines of risk, as quantified by the years when projected annual fasting period lengths exceed cub recruitment and adult survival impact thresholds in different subpopulation regions. a,**b**, Years of first impact on cub recruitment (magenta), adult male survival (blue) and adult female survival (red) are shown for the RCP4.5 (**a**) and RCP8.5 scenarios (**b**), assuming fast-initiating masses that are 20% lighter (light shade), the same (medium-light shade), 20% heavier (medium-dark shade) or 40% heavier (dark shade) than in $WH_{89\text{-}96}$. The risk of demographic impacts increases with darker colours. Demographic impacts were considered possible when fast duration exceeds the −20% threshold, likely between exceedance of the 0% and +20% thresholds, and inevitable by the time the +40% threshold is crossed (see Fig. 3 and Extended Data Fig. 8). All thresholds were calculated conservatively by assuming metabolic rates and energy-conserving strategies while fasting as in the Western Hudson Bay subpopulation. Additionally, thresholds of adult female survival were calculated conservatively by using the upper bound estimates for the survival times of females with dependent cubs (Table 1). The year of first impact was defined conservatively as the first occasion when three of the next five years exceed a fasting impact threshold, thus avoiding triggering impact forecasts on a single low-ice year. Font colours of subpopulation names correspond to their ecoregion designation: green, SIE; red, DIE; blue, CIE.

abandon the sea ice completely[31]. Moreover, once thresholds are crossed, impact curves rise steeply (Fig. 2 and Table 1), meaning that a few extremely poor ice years could lead to non-recoverable population declines before such years are the rule. Demographic impacts we did not consider (for example, litter size declines[15], increased subadult mortality[8], and mate-finding difficulties[34] resulting from unequal impact timelines between sexes; Fig. 4) are likely to occur in concert with, and potentially earlier than[8], the outlined cub recruitment and adult survival declines. Land-based feeding is unlikely to occur at scales that shift the timelines for recruitment and survival declines by more than a few years, because foods that meet the energy demands of polar bears are largely unavailable on land[5]. Indeed, polar bears occurred as far south as the Baltic Sea at the close of the Pleistocene[35], but did not move onto land or adapt otherwise when ice-free periods grew during Holocene warming—they simply disappeared from the region. Avoiding continued sea-ice decline requires aggressively mitigating greenhouse gas rise[36], and our results explicitly describe the costs to polar bears of avoiding that mitigation.

Online content

Any methods, additional references, Nature Research reporting summaries, source data, extended data, supplementary information, acknowledgements, peer review information; details of author contributions and competing interests; and statements of data and code availability are available at https://doi.org/10.1038/s41558-020-0818-9.

Received: 13 May 2019; Accepted: 22 May 2020;
Published online: 20 July 2020

References

1. Amstrup, S. C. et al. Greenhouse gas mitigation can reduce sea-ice loss and increase polar bear persistence. *Nature* **468**, 955–958 (2010).
2. Regehr, E. V. et al. Conservation status of polar bears (*Ursus maritimus*) in relation to projected sea-ice declines. *Biol. Lett.* **12**, 20160556 (2016).
3. Molnár, P. K., Derocher, A. E., Thiemann, G. W. & Lewis, M. A. Predicting survival, reproduction and abundance of polar bears under climate change. *Biol. Conserv.* **143**, 1612–1622 (2010); corrigendum **177**, 230–231 (2014).
4. Kay, J. E. et al. The Community Earth System Model (CESM) Large Ensemble Project: a community resource for studying climate change in the presence of internal climate variability. *Bull. Am. Meteorol. Soc.* **96**, 1333–1349 (2015).
5. Rode, K. D., Robbins, C. T., Nelson, L. & Amstrup, S. C. Can polar bears use terrestrial foods to offset lost ice-based hunting opportunities? *Front. Ecol. Environ.* **13**, 138–145 (2015).
6. Stern, H. S. & Laidre, K. L. Sea-ice indicators of polar bear habitat. *Cryosphere* **10**, 2027–2041 (2016).
7. Stirling, I. & Derocher, A. E. Effects of climate warming on polar bears: a review of the evidence. *Glob. Change Biol.* **18**, 2694–2706 (2012).
8. Regehr, E. V., Lunn, N. J., Amstrup, S. C. & Stirling, I. Effects of earlier sea ice breakup on survival and population size of polar bears in Western Hudson Bay. *J. Wildl. Manag.* **71**, 2673–2683 (2007).
9. Rode, K. D., Amstrup, S. C. & Regehr, E. V. Reduced body size and cub recruitment in polar bears associated with sea ice decline. *Ecol. Appl.* **20**, 768–782 (2010).
10. Rode, K. D. et al. A tale of two polar bear populations: ice habitat, harvest, and body condition. *Popul. Ecol.* **54**, 3–18 (2012).
11. Bromaghin, J. F. et al. Polar bear population dynamics in the Southern Beaufort Sea during a period of sea ice decline. *Ecol. Appl.* **25**, 634–651 (2016).

12. Lunn, N. J. et al. Demography of an apex predator at the edge of its range: impacts of changing sea ice on polar bears in Hudson Bay. *Ecol. Appl.* **26**, 1302–1320 (2016).
13. Obbard, M. E. et al. Trends in body condition in polar bears (*Ursus maritimus*) from the Southern Hudson Bay subpopulation in relation to changes in sea ice. *Arctic Sci.* **2**, 15–32 (2016).
14. Hunter, C. M. et al. Climate change threatens polar bear populations: a stochastic demographic analysis. *Ecology* **91**, 2883–2897 (2010).
15. Molnár, P. K., Derocher, A. E., Klanjscek, T. & Lewis, M. A. Predicting climate change impacts on polar bear litter size. *Nat. Commun.* **2**, 186 (2011).
16. De la Guardia, L. C., Derocher, A. E., Myers, P. G., van Scheltinga, A. D. T. & Lunn, N. J. Future sea ice conditions in Western Hudson Bay and consequences for polar bears in the 21st century. *Glob. Change Biol.* **19**, 2675–2687 (2013).
17. Hamilton, S. G. et al. Projected polar bear sea ice habitat in the Canadian Arctic Archipelago. *PLoS ONE* **9**, e113746 (2014).
18. Cavalieri, D., Parkinson, C., Gloersen, P. & Zwally, H. J. *Sea Ice Concentrations from Nimbus-7 SMMR and DMSP SSM/I-SSMIS Passive Microwave Data* Version 1 (1979–2016) (NASA DAAC at the National Snow and Ice Data Center, accessed 7 June 2017).
19. Arnould, J. P. Y. & Ramsay, M. A. Milk production and milk consumption in polar bears during the ice-free period in western Hudson Bay. *Can. J. Zool.* **72**, 1365–1370 (1994).
20. Dyck, M., Campbell, M., Lee, D. S., Boulanger, J. & Hedman, D. *Aerial Survey of the Western Hudson Bay Polar Bear Sub-Population 2016.* 2017 Final Report (Wildlife Research Section, Department of Environment, Government of Nunavut, 2017).
21. Manning, T. H. *Geographical Variation in the Polar Bear Ursus Maritimus Phipps.* Rep. Ser. No. 13 (Canadian Wildlife Service, 1971).
22. Derocher, A. E. & Stirling, I. Geographic variation in growth of polar bears (*Ursus maritimus*). *J. Zool. Lond.* **245**, 65–72 (1998).
23. Derocher, A. E. & Wiig, Ø. Postnatal growth in body length and mass of polar bears (*Ursus maritimus*) at Svalbard. *J. Zool. Lond.* **256**, 343–349 (2002).
24. Obbard, M. E. et al. Re-assessing abundance of Southern Hudson Bay polar bears by aerial survey: effects of climate change at the southern edge of the range. *Arctic Sci.* **4**, 634–655 (2018).
25. Peacock, E., Taylor, M. K., Laake, J. & Stirling, I. Population ecology of polar bears in Davis Strait, Canada and Greenland. *J. Wildl. Manag.* **77**, 463–476 (2013).
26. Galicia, M. P., Thiemann, G. W., Dyck, M. G. & Ferguson, S. H. Characterization of polar bear (*Ursus maritimus*) diets in the Canadian high arctic. *Polar Biol.* **38**, 1983–1992 (2015).
27. Laidre, K. L. et al. Interrelated ecological impacts of climate change on an apex predator. *Ecol. Appl.* **30**, e02071 (2020).
28. Stapleton, S., Peacock, E. & Garshelis, D. Aerial surveys suggest long-term stability in the seasonally ice-free Foxe Basin (Nunavut) polar bear population. *Mar. Mammal Sci.* **32**, 181–201 (2016).
29. Regehr, E. V. et al. Integrated population modeling provides the first empirical estimates of vital rates and abundance for polar bears in the Chukchi Sea. *Sci. Rep.* **8**, 16780 (2018).
30. Stirling, I., McDonald, T. L., Richardson, E. S., Regehr, E. V. & Amstrup, S. C. Polar bear population status in the Northern Beaufort Sea, Canada, 1971–2006. *Ecol. Appl.* **21**, 859–876 (2011).
31. Pagano, A. M. et al. High-energy, high-fat lifestyle challenges an Arctic apex predator, the polar bear. *Science* **359**, 568–572 (2018).
32. Aars, J. et al. The number and distribution of polar bears in the western Barents Sea. *Polar Res.* **36**, 1374125 (2017).
33. Moss, R. et al. *Towards New Scenarios for Analysis of Emissions, Climate Change, Impacts, and Response Strategies* (IPCC, 2008).
34. Molnár, P. K., Derocher, A. E., Lewis, M. A. & Taylor, M. K. Modelling the mating system of polar bears: a mechanistic approach to the Allee effect. *Proc. R. Soc. B* **275**, 217–226 (2008).
35. Ingolfsson, O. & Wiig, Ø. Late Pleistocene fossil find in Svalbard: the oldest remains of a polar bear (*Ursus maritimus* Phipps, 1744) ever discovered. *Polar Res.* **28**, 455–462 (2008).
36. Notz, D. & Stroeve, J. Observed Arctic sea-ice loss directly follows anthropogenic CO_2 emission. *Science* **354**, 747–750 (2016).

Methods

Sea-ice-free season and fast duration. Because energy-rich foods required by polar bears are largely unavailable on land[5], we assumed that fast duration is linked to the annual number of ice-free days in each subpopulation region. We computed the ice-free season from observed and modelled daily sea-ice concentrations, and linked our estimates to reported annual migration dates of polar bears in the Western Hudson Bay subpopulation to ensure that each year's first and last fasting day were defined from a polar bear's perspective. As a baseline, we assumed that ice availability–fasting relationships are similar in other subpopulations, and then quantified potential errors that may arise from associated assumptions. As in previous analyses of the sea-ice habitat use of polar bears[2,6,37,38], we derived the observed sea-ice concentration from daily PMW satellite radiometry with the NASA Team algorithm version 1.1 (ref. [18]). Historical and future projections of daily sea-ice concentration are from CESM1 with the Community Atmosphere Model version 5 (ref. [4]). There were 30 ensemble members for the historical simulations (1979–2005) and RCP8.5 simulations (2006–2100), and 14 ensemble members for the RCP4.5 simulations (2006–2080).

Sea-ice concentration values from both PMW and CESM1 are gridded. PMW grid cells are approximately 25 km × 25 km. The grid of CESM1 has a resolution of approximately 1°, with the grid converging in Greenland rather than at the true North Pole (Supplementary Fig. 1)[39]. Subpopulation regions in the AE were excluded from our analyses because resolution of both the PMW and CESM1 grids is inadequate to resolve sea-ice changes in the narrow inter-island channels accurately (Supplementary Fig. 1). Dynamical downscaling was not possible because it is computationally prohibitive for the 44 ensemble members. Statistical downscaling was also rejected because a statistical model built on past observations may be unreliable when applied many decades in the future when the sea ice is likely to be very different. Subpopulation regions in the SIE, DIE and CIE (Fig. 1) were defined according to refs. [1,40]. In the Southern Beaufort Sea subpopulation region, we excluded ocean areas deeper than 300 m from ice-free season assessments to maintain consistency with previous analyses[14,41] and account for observed food deprivation in Southern Beaufort Sea bears that remain on the sea ice after it retreats from productive near-shore waters[31,42,43].

Daily sea-ice concentration data were processed into daily sea-ice extent for the 13 subpopulation regions of the SIE, DIE and CIE. Sea ice extent is the area of all grid cells in a region where concentration exceeds a pre-specified threshold (for example, a 15% threshold is used for the well-known Sea Ice Index of the National Snow and Ice Data Center[44]). Here, we used a 30% threshold, assuming poor polar bear foraging efficiency below sea-ice concentrations of 30%. Indeed, although polar bears may use areas of low ice concentration during break-up and freeze-up (see below), capturing seals in open water is thought to be rare[45], and when available, bears seem to prefer ice concentrations greater than 50% (refs. [37,46]). Extended Data Fig. 1 illustrates our estimates of sea-ice extent from PMW data for the Western Hudson Bay region from 1979–2016.

The ice-free season was defined as the period when the extent in a subpopulation region is below a critical value. Our choice of this critical extent was based on when polar bears in the Western Hudson Bay subpopulation were observed to arrive on-shore (leaving the ice) in summer and depart the land (returning to ice) in autumn. The migration dates were assessed from bear locations tracked by satellite-linked radio collars in 1991–2009, as reported in ref. [38]. The mean days of the year of bear on-shore arrival and departure to sea ice were 212 and 329, respectively (averaged across all bears in all available years from 1991–2009; Extended Data Fig. 2). However, according to Extended Data Fig. 1, the mean sea-ice extent in Western Hudson Bay on day 212 was extremely low (3.8% of the annual maximum in the years 1991–2009), suggesting that bears may have lingered on a few persistent clusters of small, highly ridged floes, which could provide cover for aquatic stalks[45], before giving up on the ice and coming ashore. In contrast, on day 329, the extent was 48.5% of the annual maximum in 1991–2009 in the Western Hudson Bay subpopulation region. Because ice extent differed substantially between bear arrival and departure dates, we chose one critical extent that is a compromise between the two, and computed times when extent first crosses the critical value for three consecutive days in summer and fall (Extended Data Fig. 1). Then, because the fasting period is defined as the number of days between the bears' on-shore arrival in summer and their departure to sea ice in autumn, we adjusted the days of the year when critical extent is crossed by constant offsets to match the mean observed arrival/departure (and hence fast initiation/cessation) dates in the Western Hudson Bay subpopulation (Extended Data Fig. 2). In essence, offsets at the start and end of the ice-free season are estimates of how long bears will linger on the last persistent floes after the extent has fallen below the critical value, and of how long it takes the bears to return to the ice after it rises above the critical value. We sought a critical extent that allows a small offset in the autumn (consistent with polar bears eager to get back on the sea ice after a long fast) and a moderate offset in summer (suggesting that polar bears continue on-ice foraging for as long as possible).

Because the maximum sea-ice extent varies annually in some regions, it is practical to define the critical extent relative to the maximum over a reference period. We defined critical extent as 30% of the March mean in each subpopulation region during the first 10 years of the satellite record (as shown in Extended Data Fig. 1 for Western Hudson Bay), and used offsets of 27 and 3 d at the start and end of the ice-free season to match bear migration dates in Western Hudson Bay—thus estimating fasting season length as 24 d shorter than the period with ice extent below 30%. Extended Data Fig. 2 shows the start and end of the estimated fasting period for the Western Hudson Bay subpopulation, along with the observed on-shore arrival and departure-to-ice dates from ref. [38]. We note that ref. [38] also computed an ice-free season and fasting period (requiring offsets of 28 and 2.5 d, respectively), but we departed from their method of defining these periods solely based on average sea-ice concentration. Our method, based on sea ice extent, is less sensitive to large errors in concentration when the surface is melting[47,48], and only an extent-based method can differentiate between conditions where the same area of ice is made up of tightly packed floes versus conditions where floes are more separated (the former condition giving a smaller extent and therefore more likely to be below the critical extent). In effect, we account for the low likelihood that polar bears could effectively use sparse, tightly packed floes.

As a baseline, we assumed that polar bears use the sea ice similarly in all regions, and therefore used the same net 24-d offset from crossing the 30% sea-ice extent threshold for defining annual fast durations in all subpopulations. However, we recognize that ice availability–fasting relationships may differ among SIE, DIE and CIE subpopulations, and therefore also tested the sensitivity of all demographic impact estimates to this assumption. While data are lacking to reliably estimate the magnitude of potential ice use differences among SIE, DIE and CIE subpopulations, recent energetic studies[31] indicate that some bears in the Southern Beaufort Sea subpopulation (DIE) may already be in energy deficit as early as April. Moreover, fasting may be costlier for bears that remain on the sea ice relative to those that fast on land due to the increased movement costs required for counteracting ice drift[31,49] and the risks of drifting too far from land or stable sea ice[50,51]. To approximate these effects, we tested the sensitivity of all demographic impact estimates by also considering an alternative ice use scenario where fasting begins in the DIE and CIE as soon as the sea-ice extent drops below 30% (see 'Estimates of future impacts and uncertainties').

Ice-free season lengths, and hence fasting periods, were computed for each ensemble member, both for historical simulations and for RCP4.5 and RCP8.5 projections. For projections, we then computed for each ensemble member the year when the fasting period first exceeded a given fasting impact threshold. When the exceedance year occurred before the end of the simulation for all ensemble members (2100 for RCP8.5 and 2080 for RCP4.5), we took the mean across the ensemble (Fig. 4). If none of the ensemble members suggested a fast duration in excess of a fasting impact threshold, we estimated that there was no risk for that subpopulation (for example, for the Queen Elizabeth Islands under the RCP4.5 scenario; Fig. 4). When some of the ensemble members exhibited an exceedance year before the end of the simulation but others did not, we computed the ensemble mean after filling in a value of 1 year past the end of the simulation for those ensemble members that otherwise did not exhibit an exceedance within the simulation.

Given that no single critical extent gave estimates of the ice-free season that matched the observed polar bear shore arrival and departure dates from ref. [38] without offsets, we also estimated the sensitivity of our demographic impact analyses to our choice of critical extent. Our baseline was 30%, and we evaluated the sensitivity of our analyses to this choice by also considering alternative critical sea-ice extent thresholds of 20% and 40%, respectively (Supplementary Fig. 2). Furthermore, we also considered uncertainty in the projected demographic impact timelines arising from internal climate variability in the climate projections by computing the 25th to 75th percentile range of fasting season length projections from the CESM1 ensemble members (Extended Data Fig. 10). Uncertainties in both critical extent and internal variability are modest compared with the uncertainty arising from unknown bear body conditions (Fig. 4), uncertain ice availability–fasting relationships (Extended Data Fig. 6) and uncertain energy use and mass loss rates (Supplementary Fig. 3 and Extended Data Fig. 9).

Estimation of recruitment and survival impact thresholds. We used a DEB model to estimate: (1) the number of days that an individual bear of mass M_0 and length L_0 can fast before death by starvation occurs; and (2) the number of days that a female with offspring can survive without compromising lactation, and hence recruitment[52] (see 'Estimation of time to death by starvation for individual bears'). Subsequently, we estimated population-level fasting impact thresholds for recruitment and adult survival as a function of $G_{(M_0,L_0)}$(subpop,year)—a subpopulation's distribution of fast-initiating masses and lengths (M_0,L_0) in a given year (see 'Population-level recruitment and survival impact thresholds').

Estimation of time to death by starvation for individual bears. We estimated the number of days that a bear of mass M_0 and length L_0 can survive on stored energy using the body composition and DEB models of Molnár et al.[3,15,53]:

$$E_0 = \alpha\left(M_0 - \rho_{\mathrm{STR}} k L_0^3\right) \quad (1)$$

$$\underbrace{\frac{dE}{dt}}_{\substack{\text{total rate}\\ \text{of storage}\\ \text{energy loss}}} = \underbrace{-m\left(\rho_{STR}kL_0^3 + \alpha^{-1}(1-\Phi)E\right)}_{\substack{\text{energy loss rate,}\\ \text{somatic maintenance}}} \underbrace{-a\left(\rho_{STR}kL_0^3 + \alpha^{-1}E\right)^b}_{\substack{\text{energy loss rate,}\\ \text{postural costs}\\ \text{(while standing or moving)}}} \underbrace{-c\left(\rho_{STR}kL_0^3 + \alpha^{-1}E\right)^d v}_{\substack{\text{energy loss rate,}\\ \text{movement}}} \underbrace{-R\left(E,\hat{X}\right)}_{\substack{\text{energy loss rate,}\\ \text{reproduction}}} \quad (2)$$

$$E(0) = E_0$$

The body composition model (equation (1)) estimates a bear's fast-initiating energy stores (E_0) from its structural mass, $\rho_{STR}kL_0^3$, and the energy density, α, of its storage mass, $M_0 - \rho_{STR}kL_0^3$. The DEB model (equation (2)) estimates energy loss rates of a fasting adult due to somatic maintenance (where m is the energy required to maintain 1 kg lean tissue for 1 d, and Φ is the proportion of storage mass that is fat), the costs of maintaining posture while standing or walking (where a and b are the allometric constant and exponent relating body mass to energy loss rate, respectively), the additional costs of moving at average speed v (where c and d are the allometric constant and exponent relating body mass to energy loss rate, respectively) and the reproductive investment $\left(R\left(E,\hat{X}\right)\right)$. The model assumes zero energy allocation to growth (constant body length L_0) during fasting[15] (Supplementary Fig. 4), because adults have largely completed structural growth[22]. Thermoregulatory costs were also not considered, as these are minor compared with maintenance and movement costs[54,55]. Time to death by starvation (t_s) for a bear entering a prolonged fast with (M_0,L_0) was defined as the time until its energy stores drop to zero, and was calculated by estimating E_0 from (M_0,L_0) using equation (1) and then solving equation (2) for $E(t_s) = 0$ (see refs. [3,53] and Supplementary Fig. 4).

Previous versions of the body composition and DEB models had estimated model parameters using physiological data, mass loss rates of fasting adult male polar bears, and a general allometric equation describing the postural and movement costs of mammals[3,15,53]. Here, we updated these parameter estimates by replacing the general mammalian allometric curve for postural and movement costs with a newly available polar bear-specific one[56] (updating parameters a, b, c and d), and then re-estimating the costs of somatic maintenance by fitting equation (2) to repeated measures of the body mass of 12 fasting adult male polar bears (updating parameters m, α_{male} and Φ_{male}; see Supplementary Fig. 3 for details). For adult females, we assumed similar somatic maintenance costs (m) to those in males[53], and used previous sex-specific estimates of α_{female} and Φ_{female} to account for systematic body composition differences (and thus differences in metabolic requirements and times to death by starvation) among the sexes[53]. Movement rates were set to $v = 1\,km\,d^{-1}$ in all simulations, assuming that food-deprived bears reduce their activity to conserve energy but still have to fulfil some minimal movement needs (for example, occasional explorations or displacements by other bears)[57–59]. Model simulations of the updated body composition/DEB model yielded mass loss rates that fell well within the range of observations, but also suggested large parameter uncertainty that may lead to underestimated mean impacts, especially for females (Supplementary Fig. 3). We quantified this uncertainty by varying the relevant model parameters within reasonable bounds (Supplementary Fig. 3) and evaluating the resultant impacts on our demographic impact analyses (see 'Estimates of future impacts and uncertainties' and Extended Data Fig. 9).

The reproductive investment $R\left(E,\hat{X}\right)$ has not been previously estimated and was set to zero for adult males as they have no reproductive investment during fasting. We also set $R\left(E,\hat{X}\right) = 0$ for solitary adult females because survival impact threshold estimates depend primarily on those individuals that have the poorest body conditions (that is, females that will not give birth[60]). In contrast, fasting females with dependent offspring allocate energy to lactation. Their $R\left(E,\hat{X}\right)$ is determined both by their own energy stores (E) and other variables $\left(\hat{X}\right)$ such as the body condition, age and number of cubs that they are supporting[19,61,62]. Moreover, mother bears may reduce or cease milk production to favour their own survival over that of their offspring as their energy reserves decline during fasting[63]. However, thresholds of $\left(E,\hat{X}\right)$ prompting reduced lactation have not been quantified[3], so we considered the extremes of the continuum between saving all energy for survival $\left(R\left(E,\hat{X}\right) = 0\right)$ and ensuring unimpaired lactation that meets all cub demands $\left(R\left(E,\hat{X}\right) = \lambda\right)$. We set the milk energy production rate (λ) to the mean values observed for fasting females with cubs ($\lambda = 10.9\,MJ\,d^{-1}$) and yearlings ($\lambda = 2.6\,MJ\,d^{-1}$) in the Western Hudson Bay subpopulation during the late 1980s[19]. See Supplementary Table 1 for a summary of all state variables, model parameters and parameter values of the body composition and DEB models.

We did not model climate change impacts on subadult survival due to a lack of data on the energetics of growth[3]. Nor did we model possible impacts on the litter size of pregnant females due to the high sensitivity of litter size to among-subpopulation variation in the relative timing of peak feeding, ice break-up and maternity denning[15]. However, we note that litter size, as well as juvenile and subadult growth and survival, are sensitive to fast duration, and will probably be impacted earlier than adult survival under ongoing ice loss. In the Western Hudson Bay subpopulation, for example, annual subadult survival rates declined during the late 1990s and early 2000s by 0.3–0.7% for each day of earlier-than-average ice break-up[8]—notably, a decline rate that mirrors our projected beyond-threshold rates of decline in adult survival (Table 1). Moreover, DEB models previously[15] predicted that mean litter size will decline in the Western Hudson Bay subpopulation by ~22–67% from the early 1990s to 2050—a trend that may already be underway, not only in Western Hudson Bay (see ref. [20] and Table 2 in ref. [64]), but also in other SIE subpopulations[27], as expected[15]. Recognizing that our approach captures only part of the survival and reproduction declines expected with climate warming, and that our model parameter choices assume optimal energy conservation strategies that probably underestimate mass loss rates and overestimate times to death by starvation (Supplementary Fig. 3 and refs. [3,15,53]), we consider our estimated timelines for declines in polar bear populations optimistic throughout (see 'Estimates of future impacts and uncertainties').

Population-level recruitment and survival impact thresholds. The within-subpopulation distribution of (M_0,L_0) in a given year, $G_{(M_0,L_0)}$(subpop,year), determines the expected times to death by starvation (t_s) for all individuals in that year, and thus subpopulation-level fast duration thresholds beyond which recruitment and/or adult survival rates would decline rapidly. However, present and past $G_{(M_0,L_0)}$(subpop,year) distributions are unknown for most subpopulations and cannot yet be anticipated reliably for the future[3]. To overcome these data gaps, we established baseline thresholds using our $WH_{89–96}$ sample of 76 adult males, 41 solitary adult females, 61 adult females with cubs and 22 adult females with yearlings (caught non-selectively during summer on-shore fasts). Thresholds for other years and subpopulations were estimated using sensitivity analyses that ask how recruitment and survival impact thresholds may differ in subpopulations where patterns of energy gain and loss may differ and/or where bears are heavier or lighter, or longer or shorter, than $WH_{89–96}$ bears.

Captured $WH_{89–96}$ bears were aged by tooth cementum assessment[65], weighed and measured (see ref. [53] and the references therein for details). All females captured with young were lactating, except for five females with cubs and three with yearlings caught near the end of the fast (late October/early November). We estimated $G_{(M_0,L_0)}(WH_{89–96})$ by calculating each bear's body mass on 1 August (the mean on-shore arrival date during the study period) from its mass and length at the time of capture (M_C,L_C) using equations (1) and (2). $G_{(M_0,L_0)}(WH_{89–96})$ is shown in Fig. 2 and Extended Data Fig. 4 (for summary statistics, see Supplementary Table 2).

From $G_{(M_0,L_0)}(WH_{89–96})$, we estimated the expected times to death by starvation (t_s) for all solitary males and females using equation (2) (Fig. 2, Extended Data Fig. 4 and Supplementary Fig. 4). For females with offspring, we estimated upper and lower bounds for each female's t_s to bracket the uncertainties arising from uncertain reproductive investment strategies $R\left(E,\hat{X}\right)$. Upper bounds, t_s^{UB}, were estimated by assuming that all females maximize their own survival by ceasing lactation immediately upon beginning a prolonged fast ($R\left(E,\hat{X}\right) = 0$; Fig. 2c and Extended Data Fig. 4c). Lower bound estimates, t_s^{LB}, assumed full lactation until maternal death ($R\left(E,\hat{X}\right) = \lambda$; Fig. 2b and Extended Data Fig. 4b) and double as estimates of the maximum fast duration that is possible without having to compromise lactation (and hence offspring recruitment[52]).

The cumulative distribution functions of starvation times (t_s, t_s^{LB} and t_s^{UB}) were roughly sigmoidal and characterized by an approximately linear section between the 5th and 95th percentile for both sexes and all reproductive classes (Fig. 2d,e and Extended Data Fig. 4d,e). We defined the recruitment impact threshold for females with cubs or yearlings as the x-intercept of the linear regression through the 5th to 95th percentile range of the cumulative distribution function of t_s^{LB}. We defined the survival impact threshold for adult males and solitary adult females as the x-intercept of the linear regression through the 5th to 95th percentile range of the cumulative distribution function of t_s. X-intercepts of the linear regressions through t_s^{LB} and t_s^{UB} provide the possible range for the survival impact threshold of females with dependent offspring. Fasting periods exceeding the recruitment impact thresholds rapidly reduce maternal investment and hence the offspring recruitment that is necessary for population maintenance. After survival impact thresholds are exceeded, adult mortality is expected to increase by z% for each additional day of fasting, where z is the slope of the regression (Fig. 2d,e, Extended Data Fig. 4d,e and Table 1). Given that subpopulation persistence generally requires annual adult female survival rates of around 93–96% (more if reproduction is already compromised)[66], even slight exceedance of an adult female survival threshold would probably push any subpopulation into a decline at the very latest. Indeed, given that steep declines in cub recruitment, yearling recruitment and adult male survival (and thus, also the ability of females to find mates for reproduction[34,67]) are expected to occur well before adult female survival is affected, population declines are likely to occur well before adult female survival impact thresholds are crossed. All impact thresholds are defined conservatively in the sense that some bears will experience effects even with shorter fasts (Fig. 2d,e and Extended Data Fig. 4d,e).

The sensitivity of fasting impact thresholds to differences in $G_{(M_0,L_0)}$(subpop,year) was explored by adjusting the M_0 and/or L_0 of all $WH_{89–96}$ bears upward or downward by a specified percentage (Fig. 2f,g, Extended Data Fig. 5 and Supplementary Fig. 5). Scenarios ranged from all bears 20% lighter than in $WH_{89–96}$ (the −20% scenario) to all bears 40% heavier than in $WH_{89–96}$ (the +40% scenario). This encompasses the approximate range of physiologically possible body masses

for a viable population (Extended Data Fig. 7) and brackets the approximate range of mean body masses across SIE subpopulations (see 'Model hindcasts'). Similarly, we varied body lengths within a range that encompasses, and probably exceeds[21,22], the range of global among-subpopulation variation (±4% relative to $WH_{89–96}$ values; that is, a mean of about ±8 cm for females and about ±10 cm for males).

Regardless of $G_{(M_0,L_0)}$(subpop,year), the model suggests that prolonged fasting impacts cub recruitment well before any other effects are felt. Declines in the survival of yearlings, adult males and mother bears follow, before ultimately solitary adult females also begin succumbing (Table 1). Following threshold exceedance, mortality is expected to increase by 0.4–0.8% for each additional day of fasting depending on sex and reproductive status (Fig. 2, Extended Data Fig. 4 and Table 1). For cases where $G_{(M_0,L_0)}$(subpop,year) ≠ $G_{(M_0,L_0)}$ ($WH_{89–96}$), the order of recruitment and survival impacts is preserved, but threshold estimates vary approximately linearly with differences in masses and/or lengths (Fig. 2, Supplementary Fig. 5 and Extended Data Fig. 5). With a 1% decline in mean body mass, recruitment impact thresholds would be exceeded ~2–3 d (~3–4 d) earlier for females with cubs (yearlings), and survival impact thresholds would be exceeded ~3–4 d (~4–5 d) earlier for adult males (solitary adult females) (Table 1 and Supplementary Fig. 3). Differences in body length have an opposite but weaker effect, with recruitment impact thresholds of females with cubs (yearlings) exceeding ~0.6 d (~1.0 d) earlier, and the survival impact thresholds of adult males (solitary adult females) exceeding ~1.0 d (~1.4 d) earlier, for each 0.1% increase in mean length (Supplementary Fig. 3). The effects of changes in masses and lengths are approximately additive, with the effects of mass changes outweighing those of length changes (Extended Data Fig. 5).

Model hindcasts. The reliability of our forecasts depends on the accuracy of the Earth system and body composition/DEB models. Previous versions of the body composition/DEB models were validated against independent body condition and metabolic data[53], including a test on almost 1,000 bears from two subpopulations (Western Hudson Bay and Southern Hudson Bay) that showed all bears falling well within the model-predicted hard boundaries of how thin or how fat a bear can be[53]. These boundaries are critical for determining our impact thresholds (Fig. 2 and Extended Data Fig. 4), and also explained observed variations in litter sizes and ice loss-related litter size declines in Western Hudson Bay in a previous study[15]. Supplementary Fig. 3 shows that the updated DEB model captures mass loss rates in fasting and resting adult polar bears. Extended Data Fig. 3 illustrates that CESM1 projections for the lengths of annual ice-free periods either agree with or slightly underestimate the ice-free season lengths observed from PMW in nearly all subpopulations, thus again rendering our estimates of future conditions and resultant demographic impacts optimistic. Compared with individual ensemble members (as shown for one subpopulation region in Extended Data Fig. 8), the variability in the model is generally consistent with the observations in all but the Davis Strait and Barents Sea regions (not shown). These two regions in particular are probably too quiescent in the model owing to the lack of turbulent eddies resolved in the ocean. Noisier time series tend to cross thresholds earlier than smoother ones, so underestimating variability leads to a delayed, and thus more optimistic, estimate of fasting impacts.

Next, we evaluated whether DEB-estimated fasting impact thresholds, combined with sea-ice observations, broadly captured observed demographic changes across polar bear subpopulations during 1979–2016 (Fig. 3). These demographic impact hindcasts were obtained by: adjusting fasting impact thresholds to account for known and assumed among-subpopulation differences and within-subpopulation temporal trends in $G_{(M_0,L_0)}$(subpop,year); intersecting the estimated impact thresholds with estimated fast durations; and comparing modelled impacts with observed demographic changes.

Among-subpopulation comparisons of $G_{(M_0,L_0)}$(subpop,year) are straightforward within the SIE where bears are generally sampled during their on-shore fasts. Compared with Western Hudson Bay: bears in Southern Hudson Bay are assumed to be ~10% heavier (M. Obbard, unpublished data); males in Davis Strait and Foxe Basin are ~20% and ~40% heavier, respectively; Foxe Basin females are on average ~20% heavier; and Davis Strait females are about the same weight as Western Hudson Bay females (Fig. 5 in ref. [22] and Fig. 5 in ref. [68]). No comparative information exists for bears in Baffin Bay. In the Western Hudson Bay subpopulation, body masses have declined at an approximate rate of −5.7% per decade between 1980 and 2007 (Fig. 5 in ref. [7]), and we assumed similar decline rates for Southern Hudson Bay and Davis Strait, where studies have reported declining body conditions but not the mass loss rates[10,13]. In contrast, the Foxe Basin subpopulation is thought to be relatively stable[28], so we assumed no temporal trends in body mass there. Body lengths, which were similar throughout the SIE[21,22] and for which no temporal trends were reported anywhere, were assumed to equal those in $WH_{89–96}$ in all subpopulations and years. Subpopulation-specific fasting impact thresholds that account for these differences and trends were calculated for the observational period using the sensitivity approach described in the section 'Estimation of recruitment and survival impact thresholds', and are shown in Fig. 3. Intersecting the estimated fasting impact thresholds with estimated annual fast durations for 1979–2016 yielded demographic impact hindcasts that capture the timing and nature of reported demographic changes throughout the SIE (see Fig. 3 and main text).

The dearth of mass and length data for the DIE and CIE prevented estimation of baselines and trends in $G_{(M_0,L_0)}$(subpop,year) and corresponding subpopulation-specific fasting impact thresholds for these areas (see main text). Moreover, data quantifying how the ice extent–fast duration relationship may be different from what is observed in Western Hudson Bay are also lacking (see section 'Sea-ice-free season and fast duration' above). Therefore, we considered the full range of feasible body conditions (−20% to +40% of the $G_{(M_0,L_0)}$($WH_{89–96}$) baseline; Extended Data Fig. 7), and intersected all possible fasting impact thresholds with fast durations based on the two scenarios of ice use outlined in the section 'Sea-ice-free season and fast duration': (1) a fast duration that is 24 d shorter than the summer period with ice extent <30% (Fig. 3); and (2) a fast that begins as soon as extent drops below 30% (Extended Data Fig. 6). In all analyses, we assumed similar body lengths as in $WH_{89–96}$ due to conflicting reports of among-subpopulation differences. For example, Manning[21] suggested a circumpolar gradient in skeletal size from East Greenland (smallest) to Alaska (largest), whereas Derocher and Stirling[22] reported opposing patterns. However, we note that threshold crossings would occur earlier (later) than depicted in Figs. 3 and 4 and Extended Data Figs. 6 and 9 if bears in a subpopulation are generally longer (shorter) than in $WH_{89–96}$ but of similar mass (Extended Data Fig. 5).

Despite these uncertainties, demographic impact hindcasts compared favourably with observed demographic changes in all DIE and CIE subpopulations where trend data are available (see also main text). In the Southern Beaufort Sea, declining body masses[9], along with possibly larger skeletal sizes[21] and potentially larger movement costs relative to the Western Hudson Bay subpopulation[31,50], imply that thresholds may already be crossed (Extended Data Fig. 6), in agreement with observed reproduction, survival and abundance declines[11]. In contrast, in the Chukchi Sea subpopulation, stable body masses—possibly due to extraordinary marine productivity and longer summer foraging periods than in the Southern Beaufort Sea[29,68]—make it unlikely that thresholds have already been crossed, even if Chukchi Sea bears were longer than $WH_{89–96}$ bears[21] and/or more strongly affected by ice absence than SIE bears (Extended Data Fig. 6). The driving effects of body mass over body length (Supplementary Fig. 5 and Extended Data Fig. 5) may also be evident in the Barents Sea, where bears are shorter but also lighter than in Western Hudson Bay[21–23], and where, therefore, the exceedance of $WH_{89–96}$ recruitment impact thresholds (Fig. 3 and Extended Data Fig. 6) is consistent with observed low yearling numbers[32]. No data exist for the Kara Sea and Laptev Sea subpopulations. In the CIE, consistent with DEB outcomes (Fig. 3), no impacts have been observed in the Northern Beaufort Sea[30]—the only subpopulation for which demographic data exist.

Estimates of future impacts and uncertainties. We projected future demographic impact timelines by intersecting estimated impact thresholds with CESM1-based forecasts of annual fast duration (Extended Data Fig. 8 and main text). The sea-ice projections account for uncertainty due to two future scenarios and due to internal variability in the climate system. We acknowledge that relying on one model influences our estimates of fast duration, based on the results of Laliberté et al.[69]. However, we reiterate that the simulated ice-free season lengths in Extended Data Fig. 3 tend to be well matched or slightly lower than observations from 1979–2016. While the extent to which the closeness of past performance influences future projections is debated (for example, see refs. [69,70]), such close relationships are more likely to hold for demographic impacts in the next few decades. Thus, we suspect that the bias in our sea-ice projections probably contributes to an optimistic conclusion of demographic timelines that occur in the next few decades. By using just one model, we do not account for structural uncertainties in the physics and parameters of the Earth system model, but we accept this underestimate of the total uncertainty of fast duration simulated by the Earth system because we have shown that uncertainties in the demographic impact estimates are dominated by biological variables rather than the sea ice calculations. As such, we focused on quantifying the demographic forecast uncertainties resulting from unknown future body condition distributions, $G_{(M_0,L_0)}$(subpop,year), from uncertainty in the DEB model parameters, and from potential among-subpopulation differences in ice availability–fasting relationships.

The largest uncertainties stem from unknown future $G_{(M_0,L_0)}$(subpop,year) distributions, and were dealt with by considering the complete range of biologically feasible impact thresholds (−20% to +40% of $WH_{89–96}$ body masses) to define timelines of risk for when recruitment and adult survival will likely begin declining under our baseline assumptions (Extended Data Fig. 8 and Fig. 4). Uncertainties arising from uncertainty in DEB model parameters and unknown ice availability–fasting relationships were dealt with by evaluating how these timelines of risk would shift if our baseline assumptions were violated (Extended Data Figs. 6 and 9). Combined with our demographic impact hindcasts (Fig. 3), these sensitivity analyses indicate that our DEB estimates are probably accurate for males but may be underestimating impacts for females (Supplementary Fig. 3), and that impacts could occur up to 25 (RCP4.5 scenario) and 20 (RCP8.5 scenario) years earlier than projected in this case (Extended Data Fig. 9c). The estimated timelines of risk are also sensitive to assumptions regarding the ice availability–fasting relationship, with thresholds in the DIE and CIE crossed up to 32 (RCP4.5 scenario) and 24 (RCP8.5 scenario) years earlier than projected in Fig. 4, respectively, if hunting becomes impossible as soon as extent drops below 30% in summer (Extended

Data Fig. 6c). In fact, even this assumption of an early fast initiation might prove too optimistic for some subpopulations, such as the Southern Beaufort Sea, where the energy demands of walking in an increasingly fragmented sea-ice habitat can negate the energy gains from hunting and result in energy deficits well before the 30% extent threshold is crossed (that is, in cases where our energy conserving assumption of minimal movement during periods of food scarcity, $v = 1\,\mathrm{km\,d^{-1}}$, is violated)[31]. Indeed, Pagano and colleagues[31] reported that bears moving and hunting on the spring sea ice in the Southern Beaufort Sea subpopulation may have field metabolic rates that are up to four times higher than the energy usage of adult males that are fasting and minimizing movement on land in Western Hudson Bay—again rendering our baseline timelines optimistic.

We did not explicitly consider possible among-subpopulation differences in body lengths in our forecasts due to the data deficiencies outlined above, but note that the approximately linear codependence of thresholds on masses and lengths (Extended Data Fig. 5) allows implicit accounting for deviations from our baseline, with impacts hastened for longer bears and delayed for shorter bears. Changes in mass, however, remain the prevailing influence, and can occur between years. In contrast, body length declines (either due to food-stress-induced limitations to growth or evolutionary adaptations to food scarcity[71,72]) occur over longer time scales and are unlikely to substantially slow demographic impacts from declining sea ice.

In summary, and as outlined above, our timeline projections are probably conservative and predict threshold exceedance later than is likely in reality, because all model parameters and assumptions were chosen to yield optimistic estimates in cases where data scarcity necessitated a choice: we may have underestimated metabolic rates in some cases, and particularly for females (Supplementary Fig. 3); we assumed that bears do not spend energy on thermoregulation or growth and move minimally while fasting; we did not consider other demographic effects that will probably occur in concert with those outlined here, such as increased subadult mortality; and we did not consider cumulative carry-over effects among seasons. Moreover, we defined impact thresholds conservatively by using the upper bound estimates for female survival impact thresholds (Table 1 and Figs. 2 and 4), and by only considering the 5th to 95th percentile of expected starvation times for all calculations (meaning that some bears will be affected well before thresholds are crossed; Fig. 2 and Extended Data Fig. 4). Moreover, we also note that the CESM1 simulations of the length of the ice-free season slightly underestimated ice loss rates in some cases (Extended Data Fig. 3), and that years of first impact were also defined conservatively as the first occasion when three of the next five years exceed a fasting impact threshold (Fig. 4).

An empirical illustration of these points is provided by the Southern Beaufort Sea subpopulation. Annual female survival rates of at least 93% are required for population persistence with high reproduction, and higher rates are required as recruitment declines[66]. Following 297 radio-collared polar bears in the Southern Beaufort Sea for 12 years during 1981–1992 revealed an annual survival rate of 96.9% (range: 95.2–98.3%)[73]. Body condition then was good, recruitment of young was high, and the population was in a robust recovery from earlier excessive harvests[73]. In contrast, after 2000, adult female survival dropped substantially, survival of cubs was reduced by half, and the population declined steeply[11]—earlier than our timelines of risk suggested (see Fig. 4 and Extended Data Fig. 6).

Reporting Summary. Further information on research design is available in the Nature Research Reporting Summary linked to this article.

Data availability

CESM large ensemble output is available from the Climate Data Gateway at the National Center for Atmospheric Research via https://www.earthsystemgrid.org. The PMW satellite data are available from the National Snow and Ice Data Center at https://doi.org/10.5067/8GQ8LZQVL0VL. The polar bear data used in this study are available from the corresponding authors upon reasonable request.

Code availability

All analyses were conducted in MATLAB version R2016a. The computer scripts are available from the corresponding authors upon reasonable request.

References

37. Durner, G. M. et al. Predicting 21st century polar bear habitat distribution from global climate models. *Ecol. Monogr.* **79**, 25–58 (2009).
38. Cherry, S. G., Derocher, A. E., Thiemann, G. W. & Lunn, N. J. Migration phenology and seasonal fidelity of an Arctic marine predator in relation to sea ice dynamics. *J. Anim. Ecol.* **82**, 912–921 (2013).
39. Smith, R. D., Kortas, S. & Meltz, B. J. A. *Curvilinear Coordinates f or Global Ocean Models.* Tech. Note LA-UR-95-1146 (Los Alamos National Laboratory, 1997).
40. Amstrup, S. C., Marcot, B. G. & Douglas, D. C. in *Arctic Sea Ice Decline: Observations, Projections, Mechanisms, and Implications* (eds DeWeaver, E. T. et al.) 213–268 (American Geophysical Union, 2008).
41. Regehr, E. V., Hunter, C. M., Caswell, H., Amstrup, S. C. & Stirling, I. Survival and breeding of polar bears in the Southern Beaufort Sea in relation to sea ice. *J. Anim. Ecol.* **79**, 117–127 (2009).
42. Whiteman, J. P. et al. Summer declines in activity and body temperature offer polar bears limited energy savings. *Science* **349**, 295–298 (2015).
43. Whiteman, J. P. et al. Phenotypic plasticity and climate change: can polar bears respond to longer Arctic summers with an adaptive fast? *Oecologia* **186**, 369–381 (2018).
44. Fetterer, F., Knowles, K., Meier, W. & Savoie, M. *Sea Ice Index* (National Snow and Ice Data Center, 2002).
45. Furnell, D. J. & Oolooyuk, D. Polar bear predation on ringed seals in ice-free water. *Can. Field-Nat.* **94**, 88–89 (1980).
46. Stirling, I., Lunn, N. J. & Iacozza, J. Long-term trends in the population ecology of polar bears in western Hudson Bay in relation to climate change. *Arctic* **52**, 294–306 (1999).
47. Cavalieri, D. J., Parkinson, C. L., Gloersen, P., Comiso, J. C. & Zwally, H. J. Deriving long-term time series of ice cover from satellite passive-microwave multisensor data sets. *J. Geophys. Res.* **104**, 15803–15814 (1999).
48. Meier, W. N. & Stewart, J. S. Assessing uncertainties in sea ice extent climate indicators. *Environ. Res. Lett.* **14**, 035005 (2019).
49. Durner, G. M. et al. Increased Arctic sea ice drift alters adult female polar bear movements and energetics. *Glob. Change Biol.* **23**, 3460–3473 (2017).
50. Durner, G. M. et al. Consequences of long-distance swimming and travel over deep-water pack ice for a female polar bear during a year of extreme sea ice retreat. *Polar Biol.* **34**, 975–984 (2011).
51. Pagano, A. M., Durner, G. M., Amstrup, S. C., Simac, K. S. & York, G. S. Long-distance swimming by polar bears (*Ursus maritimus*) of the Southern Beaufort Sea during years of extensive open water. *Can. J. Zool.* **90**, 663–676 (2012).
52. Derocher, A. E. & Stirling, I. Aspects of survival in juvenile polar bears. *Can. J. Zool.* **74**, 1246–1252 (1996).
53. Molnár, P. K., Klanjscek, T., Derocher, A. E., Obbard, M. E. & Lewis, M. A. A body composition model to estimate mammalian energy stores and metabolic rates from body mass and body length, with application to polar bears. *J. Exp. Biol.* **212**, 2313–2323 (2009).
54. Best, R. C. Thermoregulation in resting and active polar bears. *J. Comp. Physiol.* **146**, 63–73 (1982).
55. Mathewson, P. D. & Porter, W. P. Simulating polar bear energetics during a seasonal fast using a mechanistic model. *PLoS ONE* **8**, e72863 (2013).
56. Pagano, A. M. et al. Energetic costs of locomotion in bears: is plantigrade locomotion energetically economical? *J. Exp. Biol.* **221**, jeb175372 (2018).
57. Derocher, A. E. & Stirling, I. Distribution of polar bears (*Ursus maritimus*) during the ice-free period in Western Hudson Bay. *Can. J. Zool.* **68**, 1395–1403 (1990).
58. Lunn, N. J., Stirling, I., Andriashek, D. & Richardson, E. Selection of maternity dens by female polar bears in western Hudson Bay, Canada and the effects of human disturbance. *Polar Biol.* **27**, 350–356 (2004).
59. Parks, E. K., Derocher, A. E. & Lunn, N. J. Seasonal and annual movement patterns of polar bears on the sea ice of Hudson Bay. *Can. J. Zool.* **84**, 1281–1294 (2006).
60. Derocher, A. E., Stirling, I. & Andriashek, D. Pregnancy rates and serum progesterone levels of polar bears in Western Hudson Bay. *Can. J. Zool.* **70**, 561–566 (1992).
61. Lee, P. C., Majluf, P. & Gordon, I. J. Growth, weaning and maternal investment from a comparative perspective. *J. Zool. Lond.* **225**, 99–114 (1991).
62. Oftedal, O. T. The adaptation of milk secretion to the constraints of fasting in bears, seals, and baleen whales. *J. Dairy Sci.* **76**, 3234–3246 (1993).
63. Derocher, A. E., Andriashek, D. & Arnould, J. P. Y. Aspects of milk composition and lactation in polar bears. *Can. J. Zool.* **71**, 561–567 (1993).
64. Stapleton, S., Atkinson, S., Hedman, D. & Garshelis, D. Revisiting Western Hudson Bay: using aerial surveys to update polar bear abundance in a sentinel population. *Biol. Conserv.* **170**, 38–47 (2014).
65. Calvert, W. & Ramsay, M. A. Evaluation of age determination of polar bears by counts of cementum growth layer groups. *Ursus* **10**, 449–453 (1998).
66. Regehr, E. V., Wilson, R. R., Rode, K. D. & Runge, M. C. *Resilience and Risk—a Demographic Model to Inform Conservation Planning for Polar Bears* Open-File Report 2015–1029 (US Geological Survey, 2015).
67. Molnár, P. K., Lewis, M. A. & Derocher, A. E. Estimating Allee dynamics before they can be observed: polar bears as a case study. *PLoS ONE* **9**, e85410 (2014).
68. Rode, K. D. et al. Variation in the response of an Arctic top predator experiencing habitat loss: feeding and reproductive ecology of two polar bear populations. *Glob. Change Biol.* **20**, 76–88 (2014).
69. Laliberté, F., Howell, S. E. L. & Kushner, P. J. Regional variability of a projected sea ice-free Arctic during the summer months. *Geophys. Res. Lett.* **43**, 256–263 (2016).
70. Massonnet, F. et al. Constraining projections of summer Arctic sea ice. *Cryosphere* **6**, 1383–1394 (2012).
71. McNab, B. K. Geographic and temporal correlations of mammalian size reconsidered: a resource rule. *Oecologia* **164**, 13–23 (2010).

72. McNutt, J. W. & Gusset, M. Declining body size in an endangered large mammal. *Biol. J. Linn. Soc.* **105**, 8–12 (2012).
73. Amstrup, S. C. & Durner, G. M. Survival rates of radio-collared female polar bears and their dependent young. *Can. J. Zool.* **73**, 1312–1322 (1995).

Acknowledgements

The polar bear data used in this study were collected by the late M. Ramsay of the University of Saskatchewan, and we thank F. Messier for access to these data. Dates of polar bear on-shore arrival and departure in the Western Hudson Bay subpopulation were collected and provided by A. Derocher. Sea-ice projections were produced by the CESM Large Ensemble Community Project and the CESM Medium Ensemble using high-performance computing support from Yellowstone (ark:/85065/d7wd3xhc). P.K.M. is grateful for support from a Natural Sciences and Engineering Research Council of Canada Discovery Grant (RGPIN-2016-06301), the Canada Foundation for Innovation John R. Evans Leaders Fund (grant number 35341) and the Ministry of Research, Innovation and Science Ontario Research Fund. C.M.B. is grateful for support from NOAA (grant NA18OAR4310274). M.M.H. acknowledges support from NSF. J.E.K. acknowledges start-up funds from the University of Colorado. S.R.P. is grateful for support from Polar Knowledge Canada through their Northern Scientific Training Program. S.C.A. is grateful for 30 years of research opportunity at USGS, to the staff, board and many supporters at PBI, and to the University of Wyoming.

Author contributions

S.C.A. conceived the study. P.K.M. and S.C.A. conceptualized all polar bear analyses. P.K.M. wrote the polar bear fasting model, and P.K.M. and S.R.P. performed the simulations. C.M.B. analysed the sea-ice observations. C.M.B. and M.M.H. analysed the climate model output. J.E.K. organized the climate model integrations. P.K.M., S.C.A. and C.M.B. co-wrote the paper.

Competing interests

The authors declare no competing interests.

Additional information

Extended data is available for this paper at https://doi.org/10.1038/s41558-020-0818-9.

Supplementary information is available for this paper at https://doi.org/10.1038/s41558-020-0818-9.

Correspondence and requests for materials should be addressed to P.K.M. or C.M.B.

Peer review information *Nature Climate Change* thanks Nadja Steiner and the other, anonymous, reviewer(s) for their contribution to the peer review of this work.

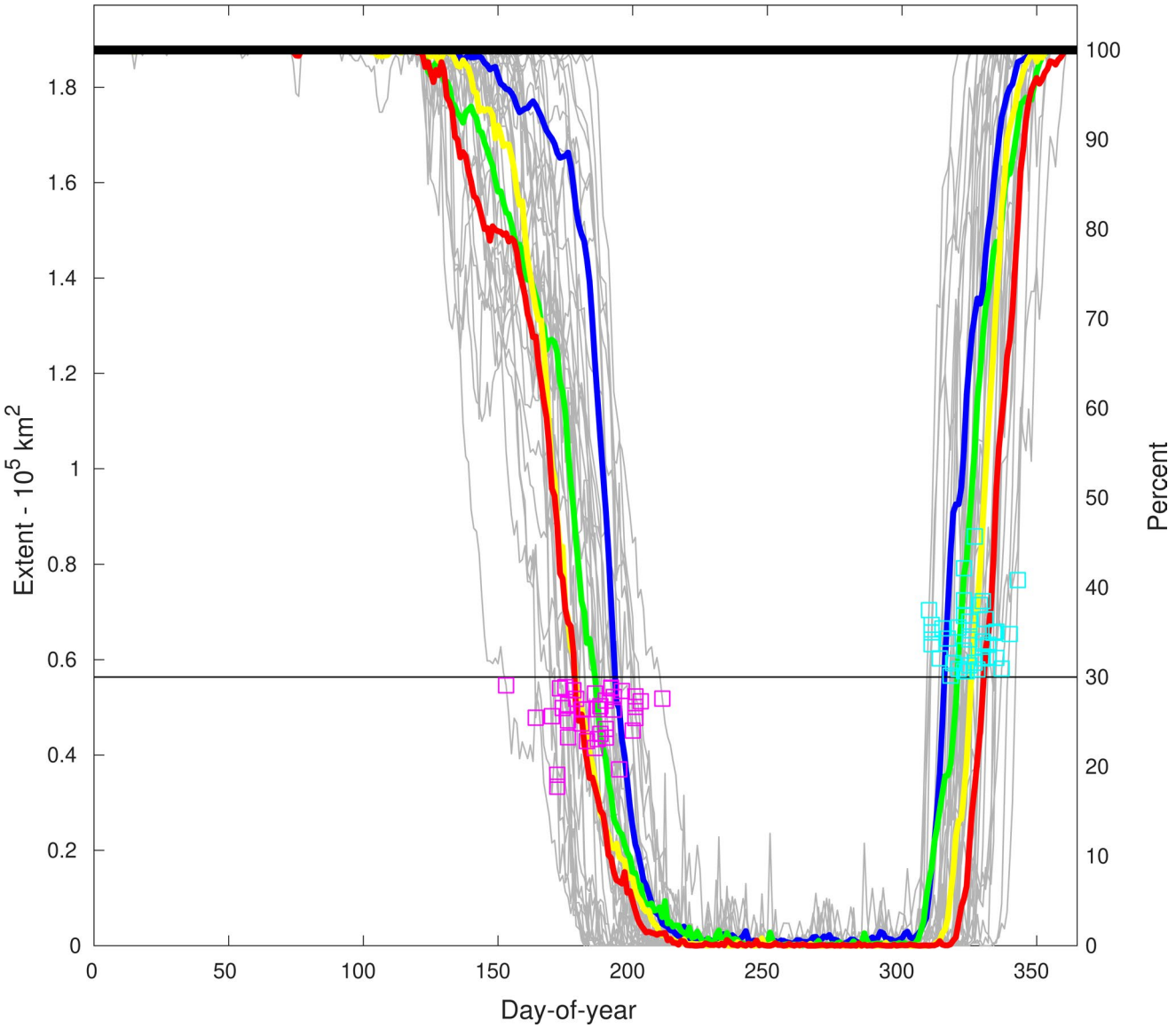

Extended Data Fig. 1 | The annual extent of sea ice in the Western Hudson Bay subpopulation region as derived from PMW data. Grey lines are daily extent in each year for 1979-2016 based on satellite observations. The colored curves are means of the daily extent: 1979-1988 (blue), 1989-1999 (green), 2000-2009 (yellow), and 2010-2016 (red). The thick black line is the 1979-1988 March mean extent, and the thin black line is the critical extent, taken as 30% of the 1979-1988 March mean. The first (last) day-of-the-year when the extent drops below (rises above) the critical extent in each year is marked with a magenta (turquoise) square.

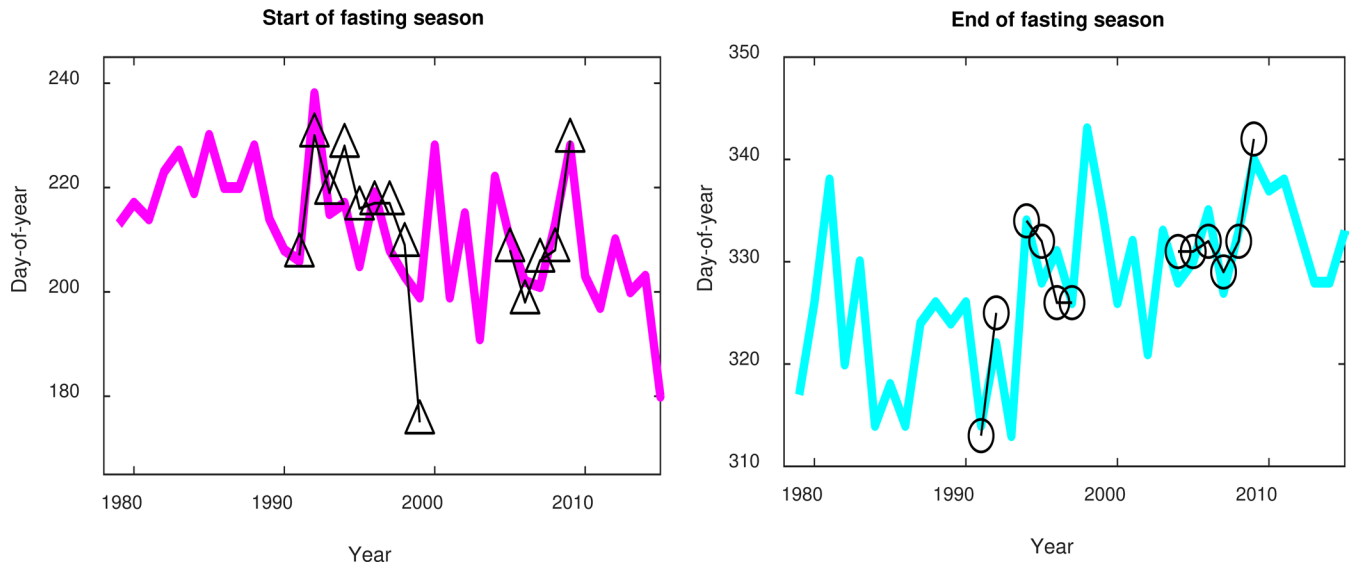

Extended Data Fig. 2 | Annual start and end day of the polar bear fasting season in Western Hudson Bay as estimated from PMW and the days-of-year when bears arrive on shore and depart back to the sea ice. Days-of-year of observed bear on-shore arrival (triangles) and departure to sea ice (circles) are from ref. [38]. The estimated start (magenta) and end (turquoise) dates of the fasting season are the days-of-year corresponding to the squares in Extended Data Fig. 1 with 27 and 3 day offsets to match the timing of the on-shore arrival and departure to sea ice of bears in Western Hudson Bay, respectively.

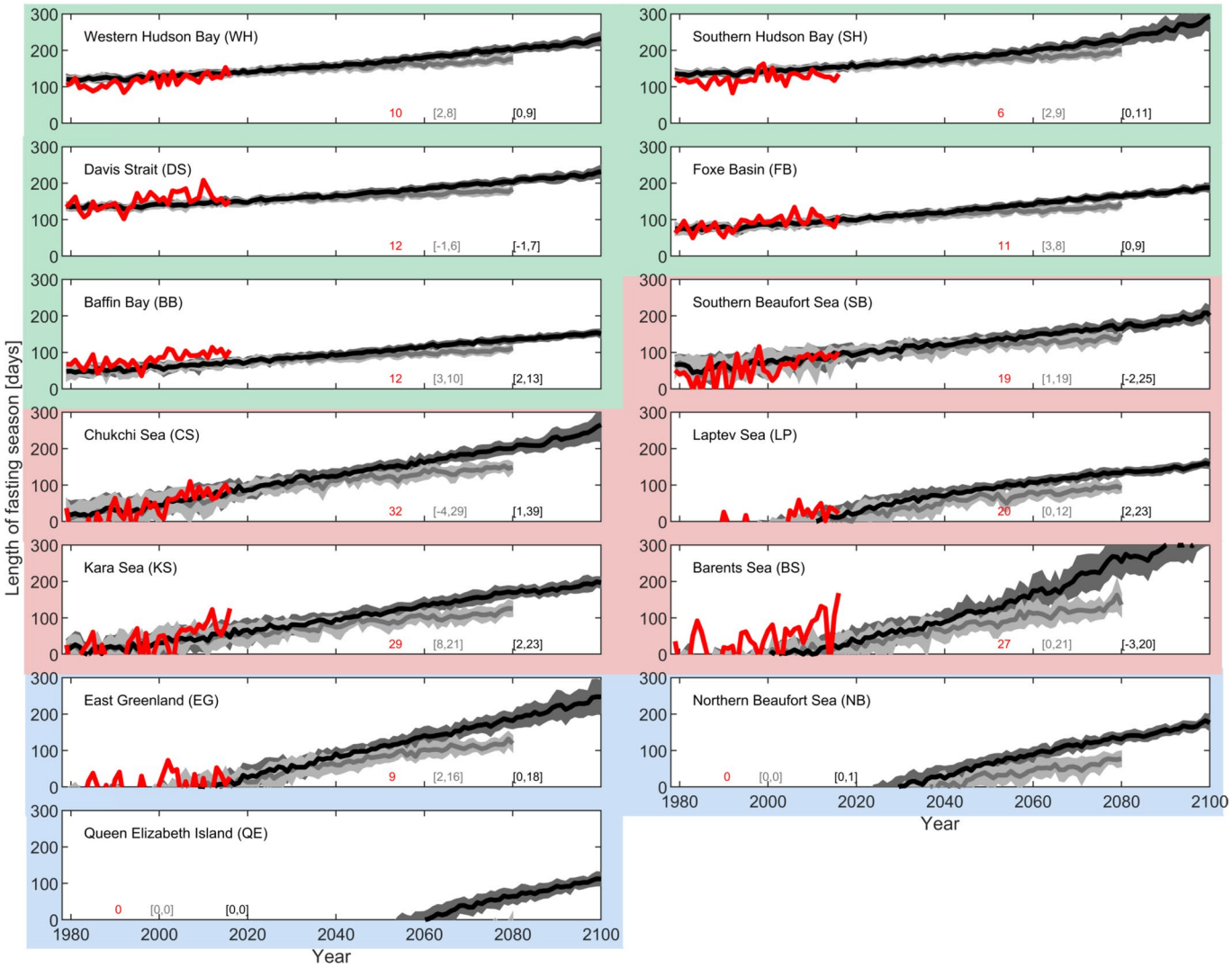

Extended Data Fig. 3 | Fasting season lengths, as estimated from PMW observations in 1979-2016 and CESM1 simulations for 1979-2100. All fasting durations were calculated as 24 days shorter than the summer period with sea ice extent <30%. Red lines are using PMW observations. Black and grey lines use the ensemble means of the CESM1 simulations with the RCP8.5 and RCP4.5 scenarios, respectively, with both having the same historical integrations through year 2005 (the RCP4.5 scenario was only run to 2080 due to computational limitations). The range of the ensemble of simulations is shown by shading plus and minus one standard deviation about the ensemble means. Numbers show the mean per-decade increase in the number of fasting days from 1979-2016, from PMW (red) and from the full range of CESM1 ensemble members (grey: RCP4.5; black: RCP8.5). Ice-free season lengths from CESM1 nearly always agree with or slightly underestimate the ice-free season lengths observed from PMW, again rendering our forecasts optimistic. Green background: SIE subpopulations; red background: DIE subpopulations; blue background: CIE subpopulations.

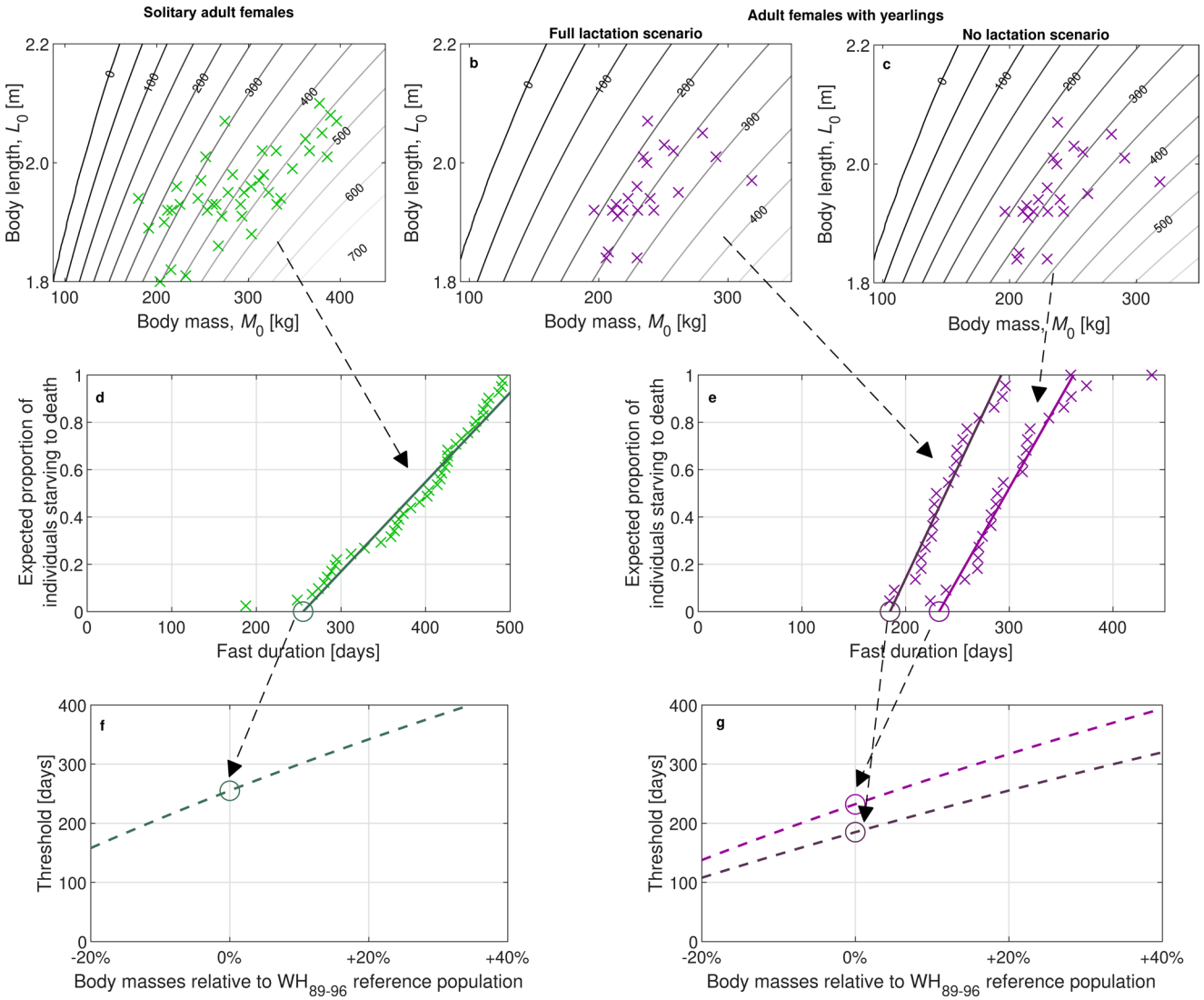

Extended Data Fig. 4 | Estimation of fasting impact thresholds for adult females without dependent offspring and for adult females with dependent yearlings. Panels follow the same logical outline as in Fig. 2, where impact threshold for adult males and adult females with cubs are estimated. (**a**-**c**) Fast-initiating masses and lengths of **a**, adult females without dependent offspring (green crosses) and of **b**-**c**, adult females with dependent yearlings (purple crosses), shown relative to DEB-estimates for the number of days to death by starvation; starvation times for females with yearlings are calculated once assuming full lactation until death (**b**), and once assuming no lactation when fasting (**c**). **d**, **e**, Cumulative distribution of estimated starvation times, and linear regressions through the 5th-95th percentile of these distributions estimating (**d**) a survival impact threshold for solitary adult females (255 days) beyond which mortality increases by ~0.4% for each additional fasting day (regression slope), and (**e**) lower (dark purple) and upper (light purple) boundaries for the survival impact thresholds of females with yearlings (185-232 days), of which the lower estimate also doubles as a yearling recruitment impact threshold. **f**, **g**, Sensitivity analyses illustrating the dependence of impact thresholds on the fast-initiating masses of bears – obtained by adjusting all WH_{89-96} masses upwards or downwards by a specified percentage within biologically reasonable bounds (cf. Extended Data Figs. 5 and 7 and Supplementary Fig. 5 for details).

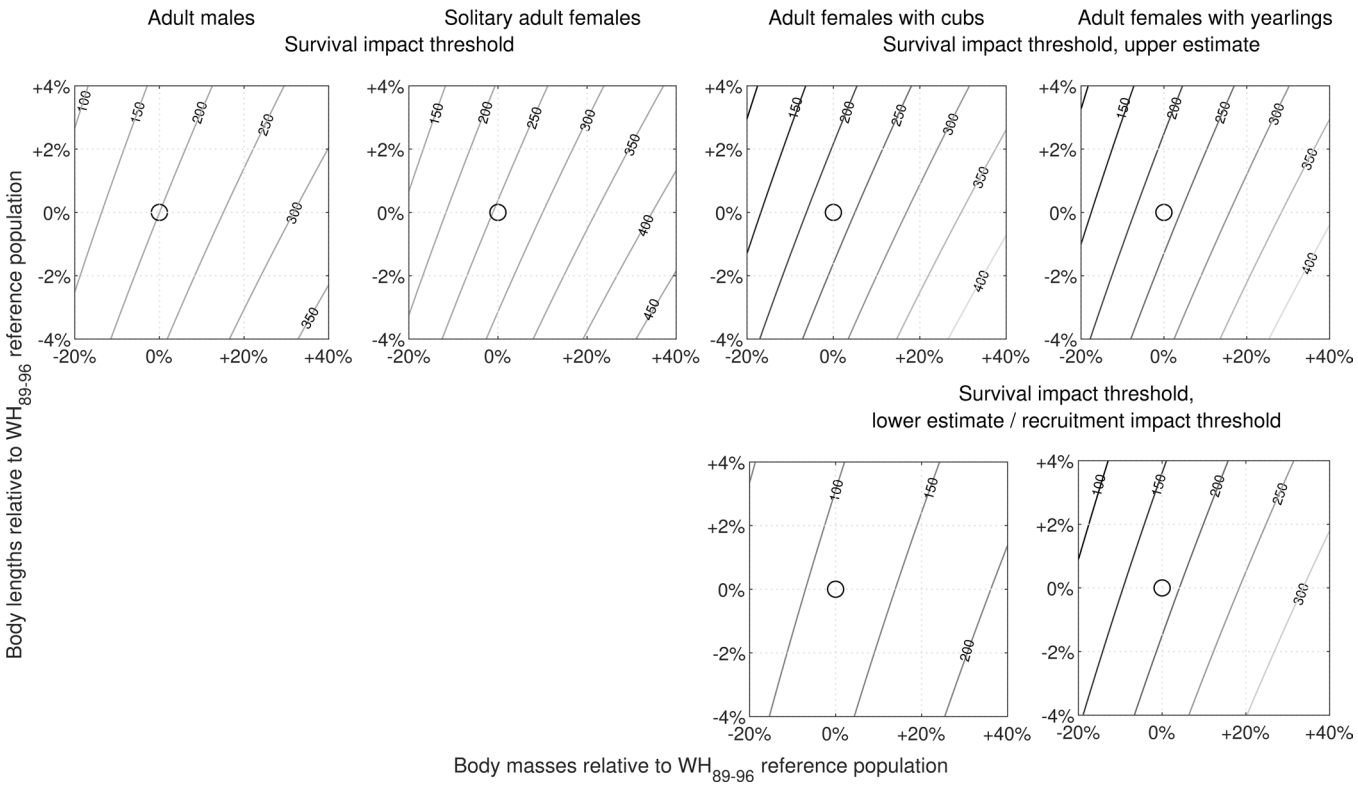

Extended Data Fig. 5 | Sensitivity of the survival and recruitment impact thresholds to changes in body mass and/or body length. The sensitivities of all survival and recruitment impact thresholds are evaluated by simultaneously adjusting the body masses and/or body lengths of all $WH_{89\text{-}96}$ bears upwards or downwards by the same percentage (cf. Supplementary Fig. 5). Contour lines show the estimated fasting impact thresholds (units: days); a circle marks the threshold estimate for each bear group in the $WH_{89\text{-}96}$ reference subpopulation.

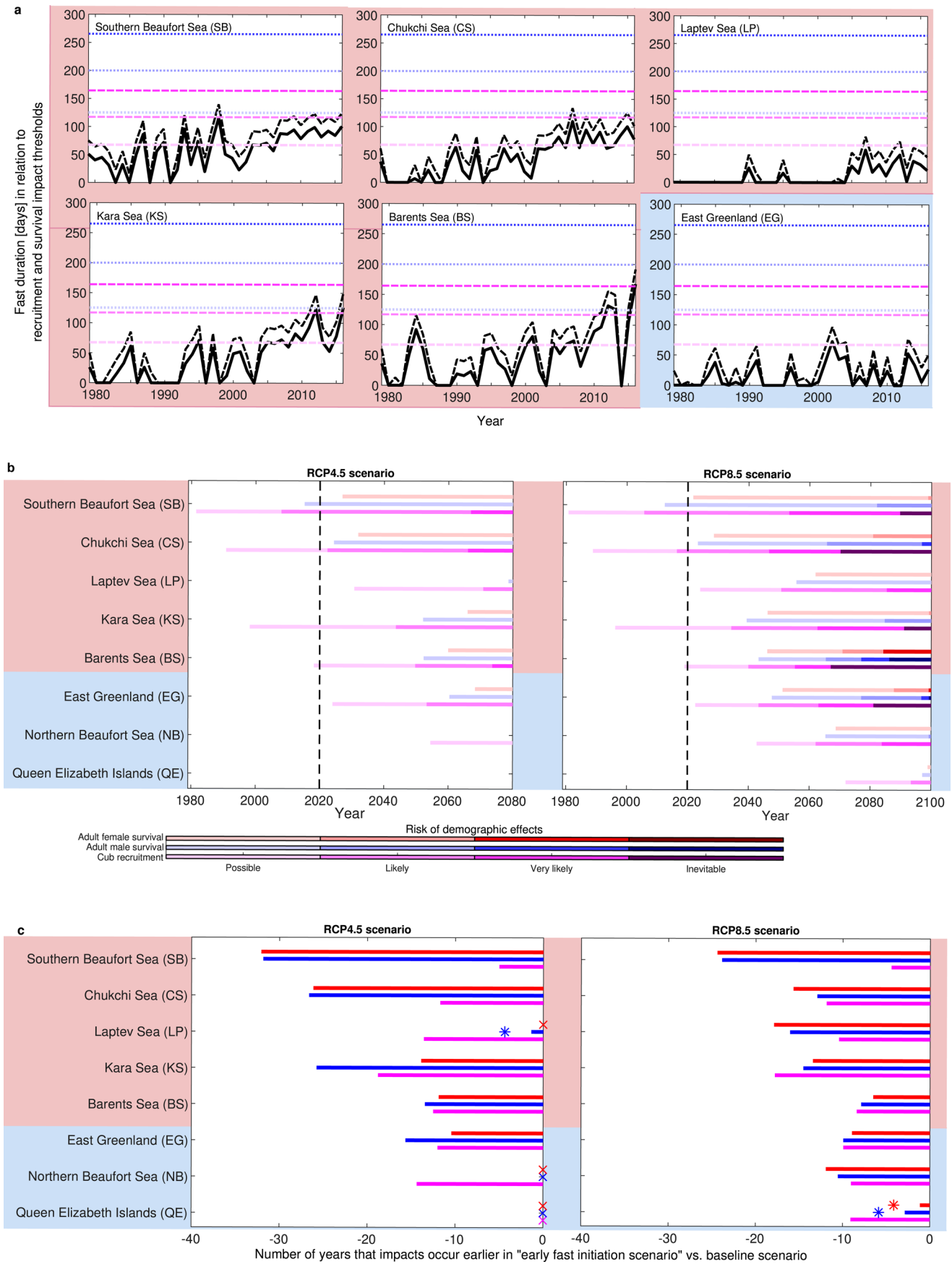

Extended Data Fig. 9 | See next page for caption.

Extended Data Fig. 6 | Sensitivity of the demographic impact analyses shown in Figs. 3 and 4 to assumptions about polar bear ice use patterns in the DIE and CIE. The baseline assumption of a 'fast duration that is 24 days shorter than the summer period with sea ice extent <30%' (as in SIE bears) is contrasted against a scenario where 'fasting begins as soon as extent <30%'. **a**, Demographic impact hindcasts as in Fig. 3; solid black line: baseline scenario, dot-dashed black line: early fast initiation; **b**, Demographic impact forecasts: as in Fig. 4, but now for the early fast initiation scenario; **c**, Difference between the baseline and early fast scenarios for the projected crossing of the first (-20%) impact threshold (that is, the difference between panel **b** & Fig. 4). Magenta: cub recruitment; blue: adult male survival; red: adult female survival. Crosses indicate cases where no impacts are predicted within the modelled timeframe for either scenario; asterisks mark cases where impacts occur with early fasting but not in the baseline, with the bar showing the minimum difference between the two scenarios in these cases. Red background: DIE subpopulations; blue background: CIE subpopulations.

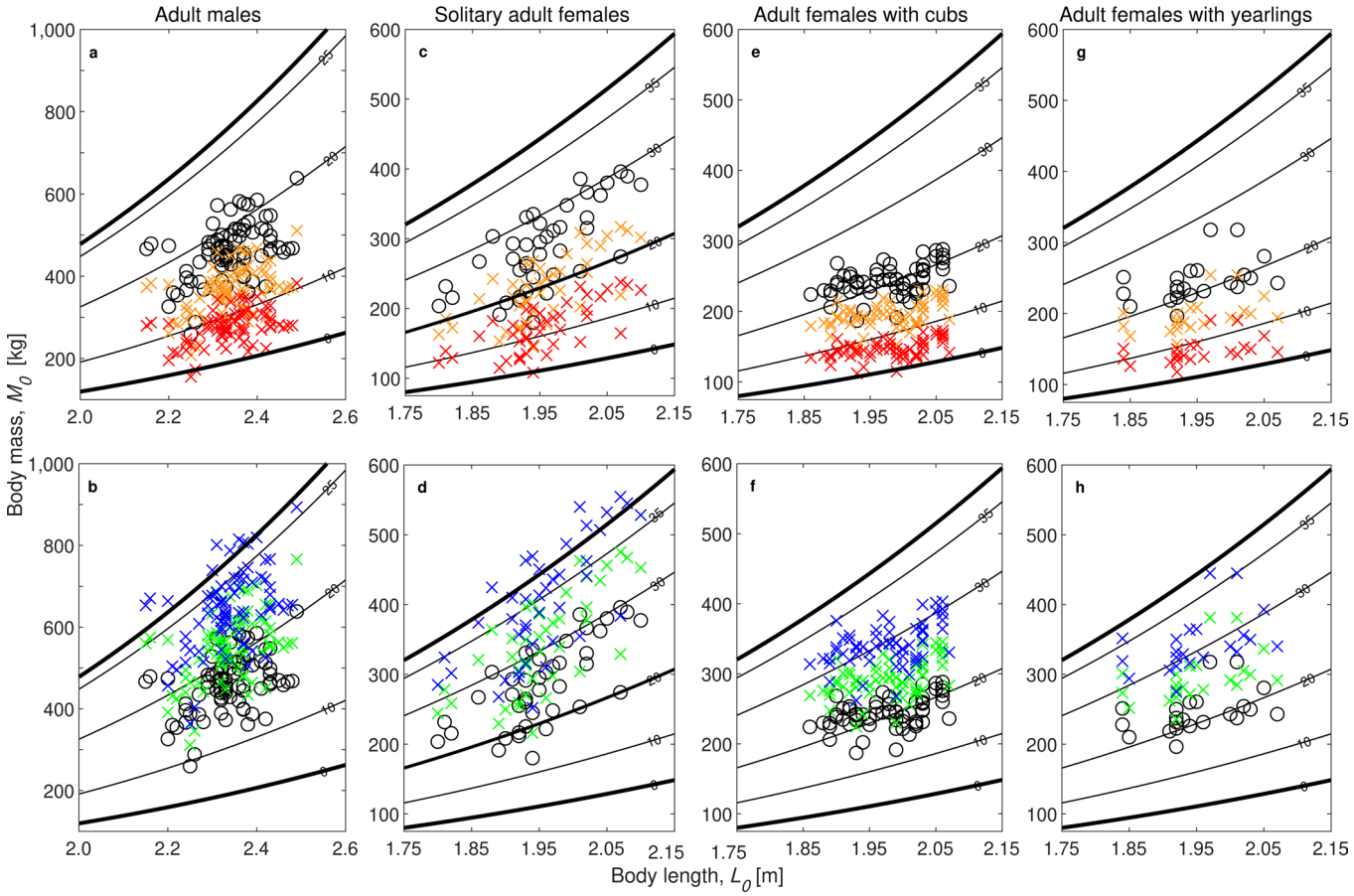

Extended Data Fig. 7 | Physiologically feasible bounds of body mass for a viable polar bear population. Contour lines show the estimated energy density of polar bears (stored energy relative to lean body mass[53]; units: MJ kg^{-1}) as a function of straight-line body length and total body mass. All bears die at zero energy density (lower thick lines) and females have never been observed to give birth if their energy density is below 20 MJ kg^{-1} before entering a maternity den[15] (middle thick lines, panels **c** and **d**). An approximate upper bound to total body mass (upper thick lines) is estimated as M=59.76L^3, which is approximately four times a bear's structural mass[53]). $G_{(M0,L0)}$(WH$_{89\text{-}96}$) is shown in each panel as black circles. Top row: all body masses decreased by 20% (orange; resulting in reproductive failure in at least half of all solitary adult females, panel **c**), and 40% (red; resulting in reproductive failure in all females); bottom row: all body masses increased by 20% (green), and by 40% (blue; resulting in unrealistically high body masses in several bears). Based on this, we conclude that the fast-initiating body masses of a viable polar bear population are likely within the −20% to +40% range of WH$_{89\text{-}96}$ values, with values at the lower (upper) end only possible if bears are simultaneously also shorter (longer), which would somewhat reduce their energetic requirements (increase their maximum possible body mass).

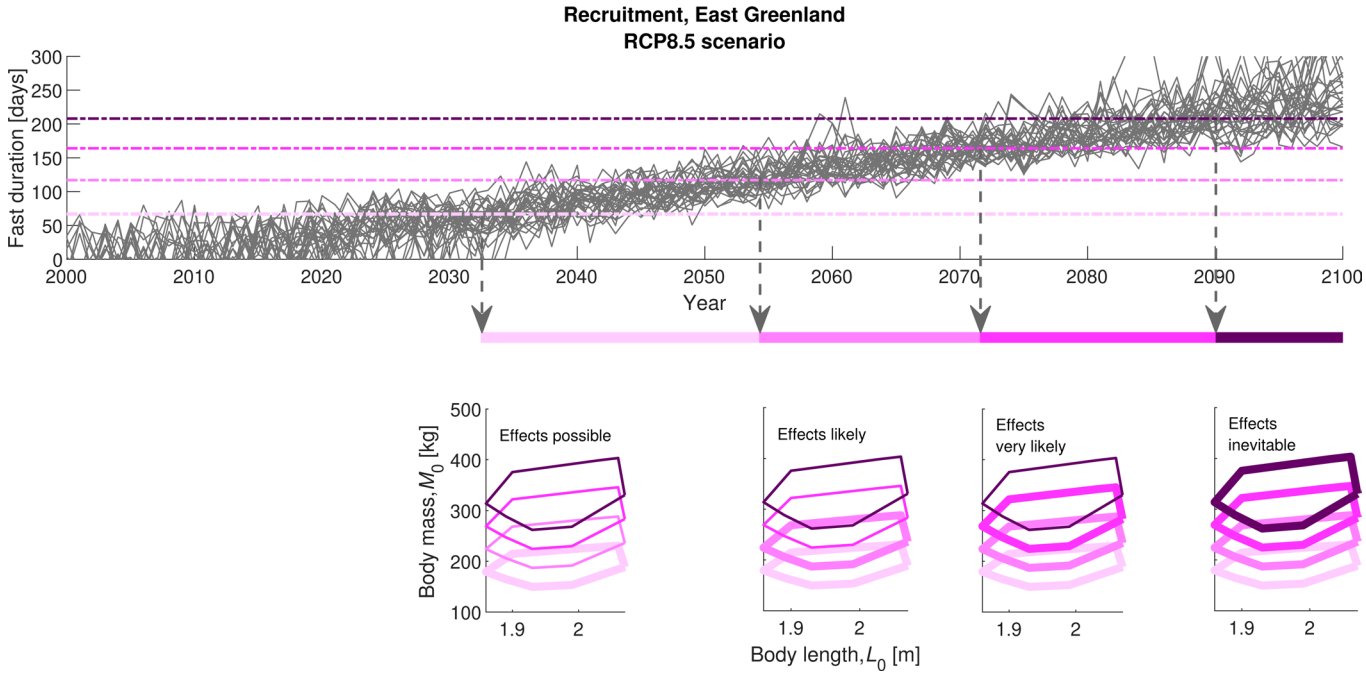

Extended Data Fig. 8 | Illustration of how timelines of risk are calculated and interpreted, using the example of recruitment in the East Greenland subpopulation (CIE) under the RCP8.5 scenario. First row shows projected fast durations till the end of the century, estimated from all thirty ensemble members of CESM1 simulations of ice-free season lengths. Horizontal lines are as in Fig. 3, showing recruitment impact thresholds, assuming masses that are 20% lower (light shade), the same (medium-light shade), 20% higher (medium-dark shade), or 40% higher (dark shade) than in $WH_{89\text{-}96}$. For each ensemble member, a threshold is defined to be crossed as the first occasion when three of the next five years exceed a fasting impact threshold, and we consider the mean across all thirty ensemble members to estimate years of first impact on polar bears. Recruitment declines are expected at a threshold crossing if the subpopulation's fast-initiating body masses fall below the corresponding value. For example, recruitment declines would be expected in 2032 if the population's $G_{(M0,L0)}$ is 20% or more below the $G_{(M0,L0)}(WH_{89\text{-}96})$ distribution in that year (vertical arrows and timeline of risk in second row). Third row: minimum convex polygons of the $G_{(M0,L0)}$-distributions for the -20% (light shade), 0% (medium-light shade), +20% (medium-dark shade), and +40% (dark shade) body mass scenarios, showing for which $G_{(M0,L0)}$-distributions recruitment declines would be expected (thick boundaries) or not (thin boundaries) at each threshold crossing. Risk increases with darker colors, both because higher body conditions are required to sustain increasingly longer fasts (contrast the four panels in third row), and because high body conditions become increasingly unlikely with longer fasts.

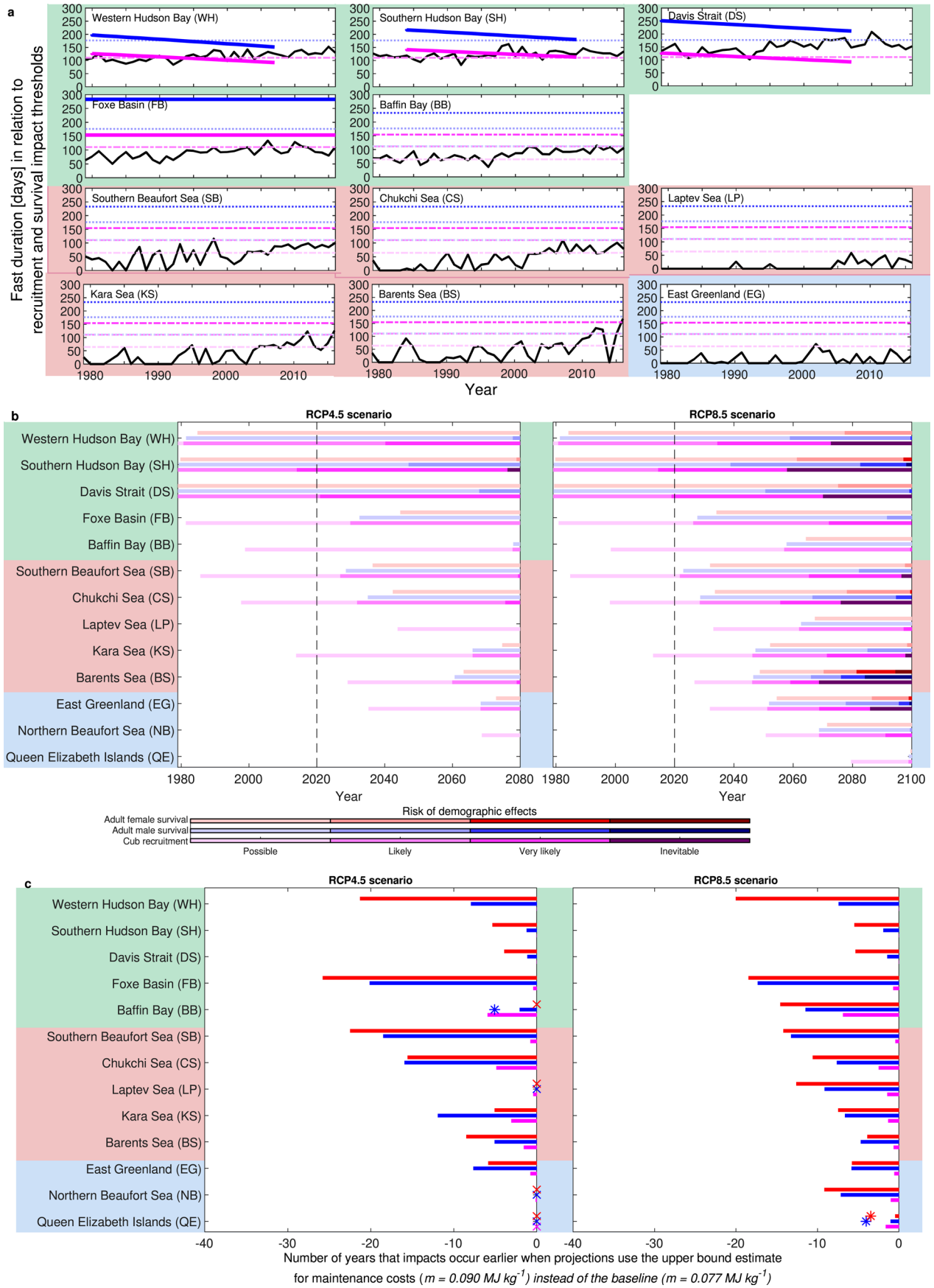

Extended Data Fig. 9 | See next page for caption.

Extended Data Fig. 9 | Sensitivity of the demographic impact analyses shown in Figs. 3 and 4 to uncertainty regarding the energetic costs of maintenance. Projections using our best estimate of $m = 0.077$ MJ kg^{-1} d^{-1} are contrasted against projections using the upper boundary estimate identified in Supplementary Fig. 3, m = 0.090 MJ kg^{-1} d^{-1}. **a**, Demographic impact hindcasts: as in Fig. 3, but now for $m = 0.090$ MJ kg^{-1} d^{-1}; **b**, Demographic impact forecasts: as in Fig. 4, but now for $m = 0.090$ MJ kg^{-1} d^{-1}; **c**, Differences between the projected crossings of the first (−20%) impact threshold when using $m = 0.090$ MJ kg^{-1} d^{-1} instead of $m = 0.077$ MJ kg^{-1} d^{-1} (that is, the difference between panel **b** & Fig. 4). Magenta: cub recruitment; blue: adult male survival; red: adult female survival. Crosses indicate cases where no impacts are predicted within the modelled timeframe using either value of m; asterisks mark cases where impacts occur with $m = 0.090$ MJ kg^{-1} d^{-1} but not with $m = 0.077$ MJ kg^{-1} d^{-1}, with the bar showing the minimum difference between the two scenarios in these cases. Green background: SIE subpopulations; red background: DIE subpopulations; blue background: CIE subpopulations.

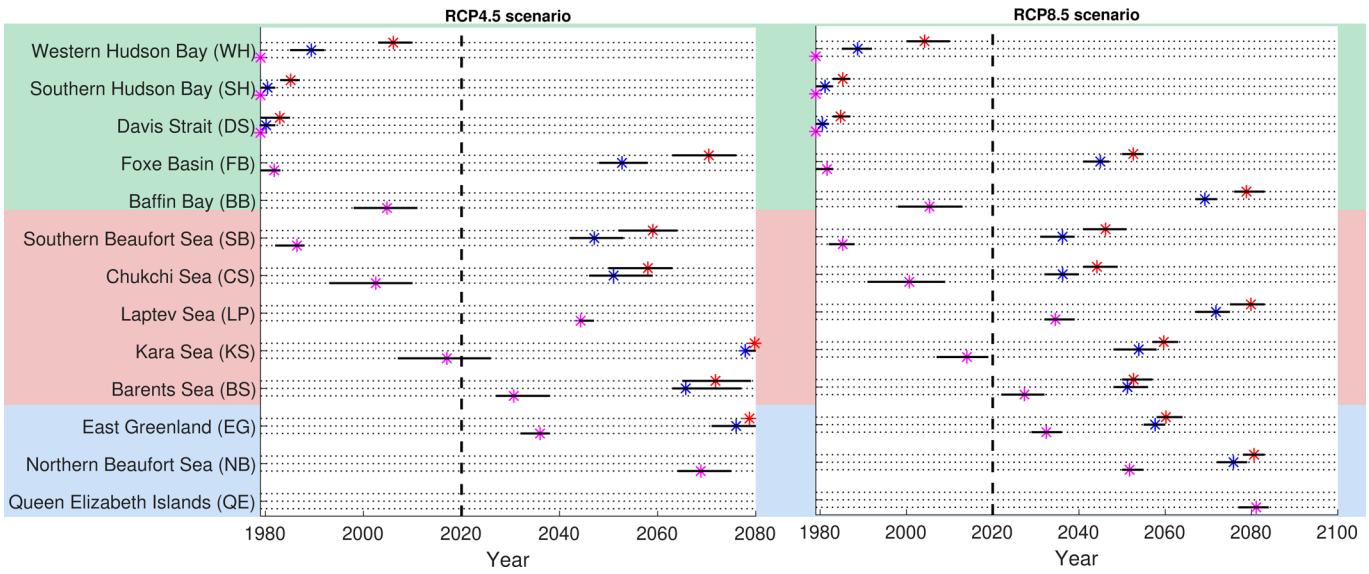

Extended Data Fig. 10 | Uncertainty of the projected demographic impacts due to climate variability. Stars show the estimated years of first impact on cub recruitment (magenta), adult male survival (blue), and adult female survival (red) from Fig. 4, that is, for our baseline assumption of a 30% critical sea ice extent threshold, and body masses, body lengths, and energy usage as in $WH_{89\text{-}96}$. Error bars around the stars illustrate the uncertainty due to climate variability by indicating the 25-75 percentile range of the earliest impact years from the CESM1 model ensembles. Year of first impact is defined as in Fig. 4.

nature research

Corresponding author(s): Peter Molnar

Last updated by author(s): Apr 23, 2020

Reporting Summary

Nature Research wishes to improve the reproducibility of the work that we publish. This form provides structure for consistency and transparency in reporting. For further information on Nature Research policies, see Authors & Referees and the Editorial Policy Checklist.

Statistics

For all statistical analyses, confirm that the following items are present in the figure legend, table legend, main text, or Methods section.

n/a	Confirmed	
☐	☒	The exact sample size (*n*) for each experimental group/condition, given as a discrete number and unit of measurement
☐	☒	A statement on whether measurements were taken from distinct samples or whether the same sample was measured repeatedly
☒	☐	The statistical test(s) used AND whether they are one- or two-sided *Only common tests should be described solely by name; describe more complex techniques in the Methods section.*
☒	☐	A description of all covariates tested
☐	☒	A description of any assumptions or corrections, such as tests of normality and adjustment for multiple comparisons
☐	☒	A full description of the statistical parameters including central tendency (e.g. means) or other basic estimates (e.g. regression coefficient) AND variation (e.g. standard deviation) or associated estimates of uncertainty (e.g. confidence intervals)
☒	☐	For null hypothesis testing, the test statistic (e.g. *F*, *t*, *r*) with confidence intervals, effect sizes, degrees of freedom and *P* value noted *Give P values as exact values whenever suitable.*
☒	☐	For Bayesian analysis, information on the choice of priors and Markov chain Monte Carlo settings
☒	☐	For hierarchical and complex designs, identification of the appropriate level for tests and full reporting of outcomes
☒	☐	Estimates of effect sizes (e.g. Cohen's *d*, Pearson's *r*), indicating how they were calculated

Our web collection on statistics for biologists contains articles on many of the points above.

Software and code

Policy information about availability of computer code

Data collection	As outlined below, we did not collect any polar bear data ourself, but rather used previously published data that were collected during the 1989-1996 population assessment of the Western Hudson Bay subpopulation and during 1991-1997 & 2004-2009 for bear migration dates. Sea ice projections were produced by the CESM Large Ensemble Community Project and the CESM Medium Ensemble using high-performance computing support from Yellowstone (ark:/85065/d7wd3xhc). Output is available on the Earth System Grid. Passive microwave satellite data are from the National Snow and Ice Data Center.
Data analysis	All analyses were conducted in MATLAB version R2016a; codes are available from the authors upon request.

For manuscripts utilizing custom algorithms or software that are central to the research but not yet described in published literature, software must be made available to editors/reviewers. We strongly encourage code deposition in a community repository (e.g. GitHub). See the Nature Research guidelines for submitting code & software for further information.

Data

Policy information about availability of data

All manuscripts must include a data availability statement. This statement should provide the following information, where applicable:

- Accession codes, unique identifiers, or web links for publicly available datasets
- A list of figures that have associated raw data
- A description of any restrictions on data availability

CESM large ensemble output is available on the Climate Data Gateway at the National Center for Atmospheric Research via https://www.earthsystemgrid.org. The passive microwave satellite data are available from the National Snow and Ice Data Center, https://doi.org/10.5067/8GQ8LZQVL0VL. The polar bear data used in this study are available from the corresponding authors upon reasonable request.

Field-specific reporting

Please select the one below that is the best fit for your research. If you are not sure, read the appropriate sections before making your selection.

☐ Life sciences ☐ Behavioural & social sciences ☒ Ecological, evolutionary & environmental sciences

For a reference copy of the document with all sections, see nature.com/documents/nr-reporting-summary-flat.pdf

Ecological, evolutionary & environmental sciences study design

All studies must disclose on these points even when the disclosure is negative.

Study description	As outlined in the manuscript, we did not collect any data for this study, but rather used data that were collected by other researchers on the body condition and migration dates of polar bears in the Western Hudson Bay subpopulation over the past decades. All data on the body condition of polar bears (body masses and body lengths) were collected by the late Malcolm Ramsay during a population assessment of the Western Hudson Bay subpopulation in 1989-1996. For this, bears were captured non-selectively in the on-shore portions of Western Hudson Bay that bears use in summer. The full dataset of this assessment was made available to the authors by Francois Messier of the University of Saskatchewan, who administered these data following M. Ramsay's death. The data were previously reported in various publications, including in our reference [53] as stated in the manuscript, where further details on the sampling procedures can be found. The full dataset of the population assessment was used in our analyses, with exclusions as described below. Dates of polar bear on-shore arrival and departure are from ref. [38] as stated in the Acknowledgments, and were provided to the authors by Andrew Derocher of the University of Alberta.
Research sample	As outlined above, the polar bear body condition data we use were collected independently by M. Ramsay and reported in previous publications, e.g. our reference [53]. The dataset consisted of 76 adult males, 41 solitary adult females, 61 adult females with cubs, and 22 adult females with yearlings.
Sampling strategy	Bears were located by helicopter and captured non-selectively following the standard protocols for population assessments. Once bears were immobilized, masses and lengths were obtained along with a series of morphometric and other measurements that are not used in this study. We do not know the details of how M. Ramsay determined sample sizes in 1989, but typically these would be set for the minimum number of bears that permit a population abundance estimate via mark-recapture techniques.
Data collection	cf. above
Timing and spatial scale	Body condition data were collected each summer from 1989-1996 during the polar bear on-shore fast from August to November by M. Ramsay and his students. Polar bear migration data were collected by Andrew Derocher and his students from 1991-1997 and 2004-2009 and were reported by them in our reference [38].
Data exclusions	All data on adult males and adult females collected during the Western Hudson Bay population assessment were used in our analyses, with the exception of three adult males and one adult female, for which either mass or length were not reported. If a bear was captured more than once during a given year, only the first capture was used in our analyses to avoid handling effects and/or pseudoreplication impacting results.
Reproducibility	As outlined above, all polar bear data are from a population assessment conducted during 1989-1996. Since these are observational rather than experimental data, they cannot be replicated. However, M. Ramsay followed standard methodologies for polar bear population assessments, so the data are comparable to subsequent assessments conducted in subsequent years.
Randomization	Polar bears were captured non-selectively by M. Ramsay following standard methodologies for polar bear population assessments. As we used the complete dataset in our analyses to fully represent population status during 1989-1996, and because these data are observational rather than experimental, randomization was not relevant to our study. Adult males, solitary adult females, adult females with cubs, and adult females with yearlings were analyzed separately due to their differing energetic requirements as outlined in the manuscript.
Blinding	As outlined above, our data are observational rather than experimental, so blinding was not relevant to our study.

Did the study involve field work? ☐ Yes ☒ No

Reporting for specific materials, systems and methods

We require information from authors about some types of materials, experimental systems and methods used in many studies. Here, indicate whether each material, system or method listed is relevant to your study. If you are not sure if a list item applies to your research, read the appropriate section before selecting a response.

Materials & experimental systems

n/a	Involved in the study
☒	☐ Antibodies
☒	☐ Eukaryotic cell lines
☒	☐ Palaeontology
☐	☒ Animals and other organisms
☒	☐ Human research participants
☒	☐ Clinical data

Methods

n/a	Involved in the study
☒	☐ ChIP-seq
☒	☐ Flow cytometry
☒	☐ MRI-based neuroimaging

Animals and other organisms

Policy information about studies involving animals; ARRIVE guidelines recommended for reporting animal research

Laboratory animals	N/A
Wild animals	As outlined above, we did not collect any data for this study, but rather used the existing data of the 1989-1996 population assessment of polar bears in Western Hudson Bay.
Field-collected samples	N/A
Ethics oversight	No ethics approval was required as we did not collect any data ourself, but rather used existing and already published data that were collected by other researchers

Note that full information on the approval of the study protocol must also be provided in the manuscript.